


# Development of an easy non-destructive particle isolation protocol for quality control of red blood cell concentrates

Marine Ghodsi<sup>1</sup> | Anne-Sophie Cloos<sup>1</sup> | Anaïs Lotens<sup>2</sup> | Marine De Bueger<sup>1</sup> |  
Patrick Van Der Smissen<sup>1</sup> | Patrick Henriët<sup>1</sup> | Nicolas Cellier<sup>2</sup> | Christophe E. Pierreux<sup>1</sup> |  
Tomé Najdovski<sup>2</sup> | Donatienne Tyteca<sup>1</sup> 

<sup>1</sup>Cell Biology Unit & Platform for Imaging Cells and Tissues, de Duve Institute, UCLouvain, Brussels, Belgium

<sup>2</sup>Service du Sang, Croix-Rouge de Belgique, Suarlée, Belgium

## Correspondence

Donatienne Tyteca, Cell biology Unit & Platform for Imaging Cells and Tissues, de Duve Institute, UCLouvain, B1.75.05, Avenue Hippocrate, 75, 1200 Brussels, Belgium. Email: [donatienne.tyteca@uclouvain.be](mailto:donatienne.tyteca@uclouvain.be)

## Abstract

The extracellular vesicle release in red blood cell concentrates reflects progressive accumulation of storage lesions and could represent a new measure to be implemented routinely in blood centres in addition to haemolysis. Nevertheless, there is currently no standardized isolation protocol. In a previous publication, we developed a reproducible ultracentrifugation-based protocol (20,000 × g protocol) that allows to classify red blood cell concentrates into three cohorts according to their vesiculation level. Since this protocol was not adapted to meet routine requirements, the goal of this study was to develop an easier method based on low-speed centrifugation (2,000 × g protocol) and limited red blood cell concentrate volumes to match with a non-destructive sampling from the quality control sampling tubing. Despite the presence of contaminants, mainly in the form of albumin and lipoproteins, the material isolated with the 2,000 × g protocol contained red blood cell-derived vesicular structures. It was reproducible, could predict the number of extracellular vesicles obtained with the 20,000 × g protocol and better discriminated between the three vesiculation cohorts than haemolysis at the legal expiry date of 6 weeks. However, by decreasing red blood cell concentrate volumes to fit with the volume in the quality control tubing, particle yield was highly reduced. Therefore, centrifugation time and relative centrifugal force were adapted (1,000 × g protocol), allowing for the recovery of a similar particle number and composition between small and large volumes sampled from the main unit, in different vesiculation cohorts over time. A similar observation was made with the 1,000 × g protocol between small volumes sampled from the quality control tubing and the mother-bag. In conclusion, our study paves the way for the use of the 2,000 × g protocol (adapted to a 1,000 × g protocol with the quality control sampling tubing) for particle measurement in blood centres.

## KEYWORDS

blood centres, Coomassie blue gel staining, extracellular particles, extracellular vesicles, nanoparticle tracking analysis, (ultra)centrifugation, Western blotting

This is an open access article under the terms of the [Creative Commons Attribution-NonCommercial](https://creativecommons.org/licenses/by-nc/4.0/) License, which permits use, distribution and reproduction in any medium, provided the original work is properly cited and is not used for commercial purposes.

© 2025 The Author(s). *Journal of Extracellular Biology* published by Wiley Periodicals LLC on behalf of International Society for Extracellular Vesicles.

## 1 | INTRODUCTION

Fresh whole blood has long been considered the gold standard for transfusion. Nowadays, at least in high-income countries, it has been replaced by the preparation and use of individual blood components. Among these, red blood cell concentrates (RCCs) represent the most commonly transfused blood product worldwide (García-Roa et al., 2017). To prepare RCCs, whole blood is collected in a bag containing citrate as anticoagulant. This bag is centrifuged to separate the blood components and squeezed to transfer red blood cells (RBCs) into a new container filled with an energetic additive solution (in Europe, Saline-Adenine-Glucose-Mannitol, SAGM). RCCs are then leucoreduced by filtration and stored at 2°C–6°C for maximum 42 days (6 weeks). However, during this period, RBCs accumulate harmful modifications, known as ‘storage lesions’ (Yoshida et al., 2019; Zimring, 2015).

Storage lesions can be classified into 3 categories: metabolic impairments, oxidative stress development, and membrane damage (Koch et al., 2019; Yoshida et al., 2019). Indeed, RBCs are suddenly exposed to a new and non-physiological environment: they are removed from plasma and resuspended in an acidic and glucose-enriched solution (SAGM), cooled, kept immobile, in contact with plasticizers, and maintained in a closed system (Zimring, 2015). Consequently, this new environment progressively induces a decrease in intracellular high-energy molecules (ATP and 2,3-diphosphoglycerate) as well as antioxidant compounds (NA(D)PH and glutathione), an extracellular accumulation of lactate and potassium, and an increase in lipid and protein oxidation. These changes can lead to the exposure of ‘death’ signals such as phosphatidylserine and clusters of Band 3, cytoskeleton reorganization and morphological alterations with a progressive release of extracellular vesicles (EVs), a loss of RBC deformability, and haemolysis (Abonnenc et al., 2018; Dinkla et al., 2014; Freitas Leal et al., 2020; Ghodsi et al., 2023; Koch et al., 2019; Kozlova et al., 2021). Metabolic alterations are generally reversible following transfusion whereas oxidative and membrane impairments are mainly irreversible (Yoshida et al., 2019). Although the potential clinical sequelae associated with transfusion of stored RCCs remain controversial (Fergusson et al., 2012; Goel et al., 2016; Lacroix et al., 2015; Lelubre & Vincent, 2013; Wang et al., 2012), storage lesions are thought to affect RBC quality, function and in vivo survival and represent a risk of adverse effects in patients (HealthCare EDftQoM, 2023; Yoshida et al., 2019; Zimring, 2015).

At Croix-Rouge de Belgique, RCC quality is routinely assessed on selected fresh products (1 day of storage) for haemoglobin (Hb) content, haematocrit (Hct) and residual leucocytes. To ensure bag sterility and integrity during these measurements, RCC volume is collected from a segment of the quality control (QC) sampling tubing (not available on all bags models). The QC sampling tubing is in contact with the inside of the unit and measures 24–28 cm. In practice, it is stripped and homogenized with the main unit. Then, a segment is sealed and detached to collect RBCs. RCC quality is also performed on a limited number of expired products for sterility and RBC integrity through haemolysis (HealthCare EDftQoM, 2023; Zimring, 2015). The latter is currently the only regulated quality parameter to assess storage lesions (Acker et al., 2018; Hess et al., 2009). It corresponds to a loss of membrane integrity that leads to the release of free Hb. As a result, haemolysis provides information about RCC ineffectiveness and risks for transfusion (D’Alessandro et al., 2010; Hess et al., 2009). Indeed, free Hb can scavenge nitric oxide, alters vasodilation, and also cause kidney damage (Rother et al., 2005; Sowemimo-Coker, 2002). To prevent these risks, Europe directives impose a legal haemolysis threshold of 0.8% at the storage expiry date (HealthCare EDftQoM, 2023). However, although easy and inexpensive to perform, the haemolysis rate is very low and only informative at the end of storage. In addition, haemolysis percentage does not fully reflect RBC functionality since stored RBCs may appear intact in RCCs but be rapidly removed from the bloodstream following transfusion. Indeed, stored RBCs have been shown to haemolyze in the patient’s circulation following transfusion or to display ‘death’ signals and be phagocytosed by macrophages in the reticuloendothelial system (Yoshida et al., 2019; Zimring, 2015).

With the growing knowledge of storage lesions, it becomes clear that other parameters, in addition to haemolysis, could be routinely measured in blood institutions to assess RCC quality. One suggestion is the measurement of EV abundance is of interest, as previously suggested by Acker and collaborators (Acker et al., 2018). This suggestion is supported by the fact that the release of EVs is the sign of the progressive accumulation of metabolic, oxidative and membrane alterations, of the loss of RBC efficiency due to their negative impact on RBC deformability, and of a risk of posttransfusion adverse effects due to their potential proinflammatory and procoagulant properties (Belizaire et al., 2012; Fischer et al., 2017; Ghodsi et al., 2023; Ma et al., 2023; Rubin et al., 2012, 2013). However, there is still no standardized protocol for isolating and measuring them. Indeed, there is a wide disparity between studies in terms of EV abundance mainly due to the use of different techniques for their concentration and analysis as well as variations of protocols when using the same technique. Among them, (ultra)centrifugation remains the gold standard for EV concentration (Nieuwland & Siljander, 2024; Théry et al., 2006). We previously developed an ultracentrifugation-based protocol to concentrate RBC-derived EVs from RCCs. We checked its reproducibility and analysed the material composition. Lipoprotein and platelet contaminants (or their vesicles) were barely detectable, while RBC and EV markers were enriched (Ghodsi et al., 2023).

Nevertheless, this ultracentrifugation protocol was not routinely applicable since: (i) it requires the acquisition of expensive ultracentrifuges, rotors and tubes, (ii) it is time-consuming and (iii) it does not preserve RCC integrity as large sample volumes are needed. Therefore, the aim of this study was to develop a simpler centrifugation-based and reliable protocol for particle recovery combined with a non-destructive RCC sampling. We also determined whether this measurement could be complementary to haemolysis used in routine tests. In accordance with the minimum requirements of the MISEV2023 publication, we used the term

'particle' when EV identity was not confirmed or when contaminants were abundant in samples (Welsh et al., 2024). Inversely, the 'EV' generic term was used for material obtained with the 20,000 × g protocol.

## 2 | MATERIALS AND METHODS

### 2.1 | RCC preparation and storage

The study was approved by the Medical Ethics Committee of the Cliniques universitaires Saint-Luc and UCLouvain (Brussels, Belgium). All donors provided written consent for the use of their donation for scientific research. Seventy RCCs from 68 different donors were prepared in PVC-DEHP bags (CompoSelect T&B 4F quadruple system, PQ32250, Fresenius Kabi) by Croix-Rouge de Belgique (Suarlée, Belgium) according to standard protocols defined by European legislations. Briefly,  $450 \pm 60$  mL of whole blood were drawn by venipuncture from volunteer donors and collected into blood bags containing 63 mL of citrate-phosphate-dextrose (CPD) solution (anticoagulant). Whole blood units were rapidly cooled and maintained at 18°C–22°C overnight. Next, RBCs were separated from plasma and buffy coat by centrifugation at  $4,000 \times g$  for 10 min, resuspended in 100 mL of SAGM additive solution, leucoreduced by filtration, and rapidly stored at 2°C–6°C at Croix-Rouge. Due to limited RCC supplies in the blood centre, not all donations could be included in the study directly after preparation. Among the 70 RCCs, 12 were delivered freshly (dark blue in Figure 1, blue lines in Table S1) while the other 58 were stored at Croix-Rouge for 1 week (w) ( $n = 6$ ), 2w ( $n = 3$ ), 3w ( $n = 17$ ), 4w ( $n = 20$ ), 5w ( $n = 4$ ) or 6w ( $n = 8$ ) before delivery to our laboratory (purple in Figure 1). Once received, all RCCs continued their storage at 2°C–6°C in our laboratory for up to 10w maximum and were evaluated for abundance, size, protein composition and morphology of EV or particle preparations as well as for RBC number and haemolysis (Figure 1, Table S1). Each RCC received an internal code corresponding to the order of entry into the study. Moreover, donor's sex, blood group and age were recorded. All information is listed in the Table S1. Out of the 70 RCCs: (i) 69 were used for both particle and EV measurement, (ii) one was only evaluated for comparison of particle abundance after sampling from the mother-bag or a segment of the QC sampling tubing, (iii) four originated from the same two donors (two RCCs from a single donor; yellow and red lines in Table S1) at 1- or 2-years intervals, and (iv) 45 RCCs were returned to Croix-Rouge for sterility control at the end of storage, which revealed no bacterial contamination.

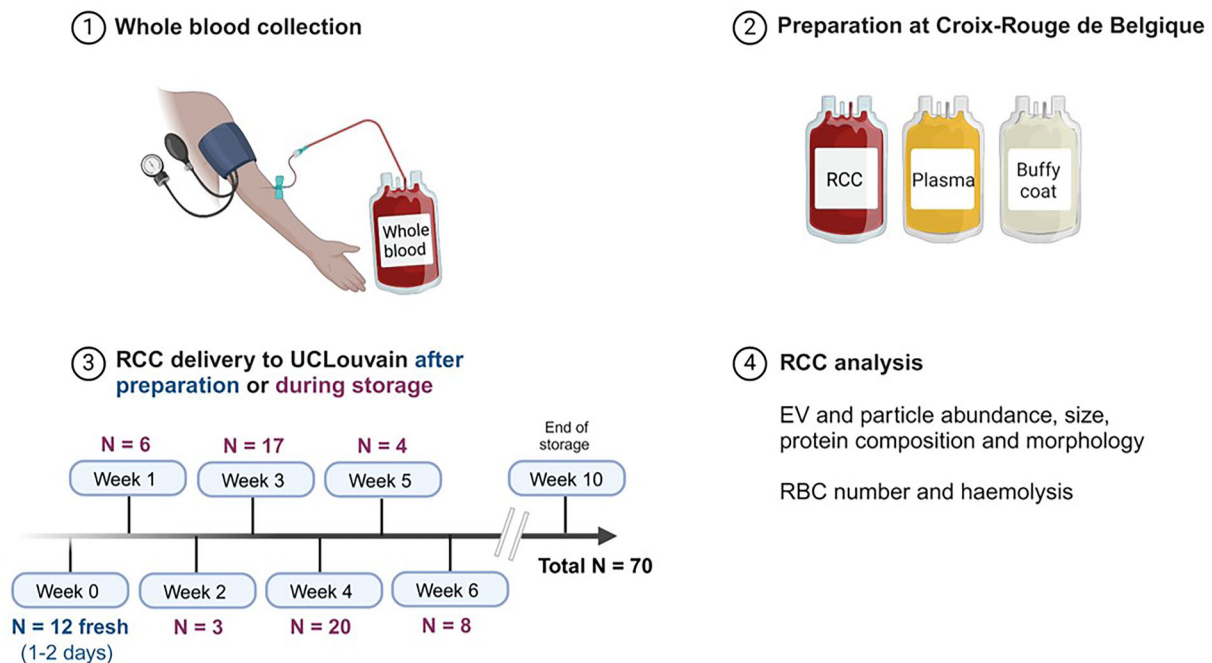


**FIGURE 1** Schematic representation of the study design and data analysis. (1) Whole blood collection. Whole blood was drawn by venipuncture from volunteer donors and collected into PVC-DEHP blood bags. (2) Preparation of red blood cell concentrates (RCCs). Red blood cells (RBCs) were isolated from plasma and buffy coat, leucoreduced and resuspended in an additive solution at Croix-Rouge. (3) RCC delivery to UCLouvain after preparation or during storage. Due to limited RCC supplies in the blood centre, 12 entered the study directly after preparation while the other 58 were stored at Croix-Rouge for 1 week (w) ( $n = 6$ ), 2w ( $n = 3$ ), 3w ( $n = 17$ ), 4w ( $n = 20$ ), 5w ( $n = 4$ ) or 6w ( $n = 8$ ) before delivery to our laboratory (total  $n = 70$  RCCs). Once received, all RCCs continued to be stored for up to a maximum of 10w. (4) RCC analysis. RCCs were evaluated for the abundance, size, protein composition and morphology of EV or particle preparations, as well as for RBC number and haemolysis. Created in BioRender. Tyteca, D. (2025) <https://BioRender.com/w81z697>.

## 2.2 | Particle and EV isolation

RBC units were gently mixed by inversion before collecting 8–10 mL (large volumes, Figure 2a) or 0.5 mL (small volumes, Figure 7d) of RCCs. When bag integrity was not maintained, the QC sampling tubing was opened to gain direct access to the inside of the bag. After collecting a certain volume of RCC, it was closed with a clamp. In contrast, to preserve RCC integrity, the QC sampling tubing was stripped and homogenized three times with the main bag. Then, a segment was sealed, detached and finally opened to collect the volume of RCC needed (Figure 9c). RCC volumes were then respectively centrifuged at  $2,000 \times g$  for 15 min ( $2,000 \times g$  protocol, Figure 2a) and  $1,000 \times g$  for 5 min ( $1,000 \times g$  protocol, Figure 7d) at  $20^\circ\text{C}$  using a Sigma 4-16Ks centrifuge (Sigma) with a swing-out rotor (11150) and buckets (13350). With this type of rotor, RBC pellet is flat, facilitating the collection of the supernatant (SP). Next, the maximum volume of SP, generally 2–3 mL (for large volumes with the  $2,000 \times g$  protocol) or 80  $\mu\text{L}$  (for small volumes with the  $1,000 \times g$  protocol), was submitted to a second centrifugation using the same parameters ( $2,000 \times g$  for 15 min for large volumes and  $1,000 \times g$  for 5 min for small volumes). The material was directly analysed for particle abundance and size and then stored at  $-80^\circ\text{C}$  for Western blotting and Coomassie blue gel staining analyses ( $2,000 \times g$  and  $1,000 \times g$  protocols). The SP obtained with the  $2,000 \times g$  protocol was also used freshly to concentrate EVs ( $20,000 \times g$  protocol, Figure 2a), as follows. Before ultracentrifugation steps, 800  $\mu\text{L}$  of SP were diluted in 7 mL of sterile phosphate-buffered saline (PBS, Cytiva, SH30256.02) solution and centrifuged at  $2,000 \times g$  at  $20^\circ\text{C}$  for 10 min (Momen-Heravi et al., 2013). The resulting SP was submitted to ultracentrifugation at  $20,000 \times g$  at  $4^\circ\text{C}$  for 20 min using the Optima XPN-80 ultracentrifuge (Beckman Coulter) with the fixed-angle Ti50 rotor. After EV resuspension in 7 mL of PBS, samples were submitted to a second ultracentrifugation step under the same conditions ( $20,000 \times g$  at  $4^\circ\text{C}$  for 20 min). The final pellet was resuspended either in 1 mL of PBS and freshly analysed for EV abundance and size or in 250  $\mu\text{L}$  of RIPA 1x lysis buffer (50 mM Tris pH 8 (VWR; 28811.295), 150 mM NaCl (Merck; 155750), 0.5% sodium deoxycholate (Merck; K48578060 715), 0.1% sodium dodecyl sulphate (SDS, Merck; 113760), 1% Triton X-100 (Serva; 37240.01), 1 mM phenylmethylsulphonyl fluoride (PMSF, Sigma-Aldrich; 78830), cOmplete™ Protease Inhibitor Cocktail (Roche; 11836145001)) as in (Ghodsi et al., 2023), and stored at  $-80^\circ\text{C}$  for Western blotting and Coomassie blue gel staining analyses. All steps were carried out in a fume hood to avoid bacterial and dust contaminations. Below is a summary of each protocol:

Steps	$2,000 \times g$ protocol	$1,000 \times g$ protocol	$20,000 \times g$ protocol
1. Gentle mix of RCCs	Yes	Yes	Yes
2. Collection of RBCs	8–10 mL	0.5 mL	8–10 mL
3. Centrifugation ( $20^\circ\text{C}$ )	$2,000 \times g$ – 15 min	$1,000 \times g$ – 5 min	$2,000 \times g$ – 15 min
4. Recovery of supernatant	2–3 mL	80 $\mu\text{L}$	2–3 mL
5. Centrifugation ( $20^\circ\text{C}$ )	$2,000 \times g$ – 15 min	$1,000 \times g$ – 5 min	$2,000 \times g$ – 15 min
6. Recovery of supernatant	For analyses and for $20,000 \times g$ protocol	For analyses	800 $\mu\text{L}$ from the $2,000 \times g$ protocol
7. Dilution of supernatant in PBS	No	No	800 $\mu\text{L}$
8. Centrifugation ( $20^\circ\text{C}$ )	No	No	$2,000 \times g$ – 10 min
9. Transfer of supernatant in ultracentrifuge tube	No	No	Yes
10. Ultracentrifugation ( $4^\circ\text{C}$ )	No	No	$20,000 \times g$ – 20 min
11. Pellet wash and resuspension	No	No	Yes
12. Ultracentrifugation ( $4^\circ\text{C}$ )	No	No	$20,000 \times g$ – 20 min
13. Pellet wash and resuspension	No	No	In PBS or RIPA 1x

## 2.3 | Particle and EV abundance and size

Particles or EVs were diluted 1:4 to 1:20,000 in PBS depending on the initial sample concentration and then measured by Nanoparticle Tracking Analysis (NTA) with a ZetaView TWIN instrument (Particle Metrix) using a blue laser (488 nm). Measurements were taken at 11 focal positions through the sample cell with the following parameters: camera sensitivity: 70; shutter: 100; minimum brightness: 30; min area: 10; max area: 10,000; resolution: medium. The concentration was then converted into a number/RBC by considering the volume of SP engaged and the average number of RBCs/ $\mu\text{L}$  in RCCs. The above settings follow the manufacturer's recommended guidelines for the detection of biological material in a size range of 70–400 nm.

## 2.4 | Coomassie blue staining of proteins

Protein content was first assessed by the Bicinchoninic acid assay (BCA) method. For the comparison of samples obtained with the  $2,000 \times g$  (particles) or  $20,000 \times g$  (EVs resuspended in RIPA 1x lysis buffer) protocols and the follow-up over time of particle samples of the three vesiculation cohorts, an equal amount of proteins (6  $\mu\text{g}$ ) was loaded onto polyacrylamide gels. In contrast, for the follow-up over time of EV samples of two RCCs from the medium vesiculation cohort, a maximum volume was loaded at 1 and 3w of storage and 3  $\mu\text{g}$  of proteins at 6w. RBC ghosts were loaded in increasing quantities (2, 4 and 6  $\mu\text{g}$ ) or 6  $\mu\text{g}$ , and used as an internal control to identify and assess the abundance of specific RBC proteins in particle and EV samples. All samples were diluted five-fold in Pierce Lane Marker Reducing Sample Buffer 5X (ThermoFisher, 39000) containing 5% SDS and 100 mM dithiothreitol and loaded onto 4%–15% Mini-Protean TGX Precast polyacrylamide gel (Bio-Rad, 4561084). After sample migration, gels were rinsed in distilled water for 2 min while shaking gently. Then, they were heated in a microwave oven until boiling and cooled for 4 min at room temperature (RT) under agitation. This step was reproduced three times in total. Water was replaced by a sufficient volume of PageBlue™ protein staining solution (ThermoFisher Scientific, 24620) to recover gels. They were once again heated to boiling and then cooled at RT for 20 min with gentle shaking. After three rapid washings in distilled water, proteins were revealed and gels were photographed. Protein quantification was performed by surrounding major bands observed on gels and determining their mean gray value (MGV) with the Fiji software. After background subtraction, the MGV was corrected by its area. To assess the total protein content, the sum of all the bands was calculated. To determine the proportion of RBC proteins compared with contaminants, a ratio was established between the sum of MGVs for RBC proteins and the sum of MGVs for ‘non-RBC’ bands.

## 2.5 | Western blotting

Equal amount (6  $\mu\text{g}$ ) of EV (resuspended in RIPA 1x lysis buffer) or particle proteins, except for plasma (6 or 20  $\mu\text{g}$ ), platelet lysates (5  $\mu\text{L}$ ) and RBC ghosts (1 or 6  $\mu\text{g}$ ), was loaded onto gels and handled as for Coomassie blue staining of proteins. After migration, proteins were transferred to polyvinylidene fluoride (PVDF) membranes. These were blocked for 2 h in 5% skim milk powder or 3% bovine serum albumin (BSA; Biowest, P6154) in Tris-buffered saline (20 mM Tris pH 7.5 (VWR; 28811.295), 500 mM NaCl (Merck; 155750)) and 0.05% Tween 20 (VWR; 28829.296) detergent (TBS-T) and probed overnight with specific primary antibodies, that is, anti-albumin (Santa-Cruz Biotechnology, sc-271604; 1:1000), anti-apolipoprotein B100 (ApoB100; Santa-Cruz Biotechnology, sc-13538; 1:500), anti-apolipoprotein A1 (ApoA1; Santa Cruz Biotechnology, sc-376818; 1:500), anti-CD41 (Abcam, ab134131; 1:2000), anti-CD45 (Santa Cruz Biotechnology, sc-1178; 1:500), anti-glycophorin A (GPA; Merck, MABF758; 1:1000), anti-Band 3 (Invitrogen, MA1-20211; 1:4000), anti-flotillin-1 (BD Biosciences, BD610820; 1:500), and anti-stomatin (Novus Biologicals, NBP2-42660; 1:1000). All antibodies were diluted in TBS-T/5% milk except for anti-CD41 in TBS-T/3% BSA. After washings, secondary peroxidase-conjugated goat anti-rabbit (Sigma-Aldrich, A0545) or anti-mouse IgGs (Invitrogen, G-21040) were incubated for 1 h and washed. Signal revelation was performed with SuperSignal™ West Pico PLUS Chemiluminescent Substrate (ThermoFisher Scientific, 34580) or SuperSignal™ West Femto Maximum Sensitivity Substrate (ThermoFisher Scientific, 34096) with Fusion Solo S (Vilber). Stripping was performed on one membrane (ApoA1, Figure 8b). To this end, the membrane was incubated with ReBlot Plus Strong Antibody Stripping Solution 1x (Merck, 2504) at RT for 25 min under agitation. After washings, membranes were blocked and probed with primary and secondary antibodies as described above. Protein quantification was performed as for Coomassie blue staining of proteins except that the corrected MGV was normalized by the number of particles in the gel. When visible, dimers were also quantified. The table below corresponds to the amount of proteins introduced into the gels of the Figure 4d.

Proteins	Plasma ( $\mu\text{g}$ )	RBC ghosts ( $\mu\text{g}$ )	$2,000 \times g$ protocol ( $\mu\text{g}$ )	$20,000 \times g$ protocol ( $\mu\text{g}$ )
Albumin	6	6	6	6
ApoB100	20	1	6	6
ApoA1	20	1	6	6
CD41	20	1	6	6
CD45	20	6	6	6
GPA	20	1	6	6
Band 3	20	6	6	6
Flotillin-1	20	1	6	6
Stomatin	20	1	6	6

## 2.6 | Electron microscopy

Freshly isolated EVs and particles were immobilized on poly-L-Lysine (Merck, P4707)-coated coverslips at RT for 8 min, washed with 0.1 M cacodylate, fixed with 1% glutaraldehyde in 0.1 M cacodylate, critical-point dried, sputter-coated with 10 nm of gold and finally observed with a CM12 electron microscope with a SED detector at 80 kV, as in (Cloos et al., 2020).

## 2.7 | RBC number and haemolysis

The number of RBCs was measured in samples collected from three RCCs before 6w and five RCCs after 6w using a haematological analyser (XN-1000, Sysmex) in Cliniques universitaires Saint-Luc. Haemolysis was measured in 29 RCCs at Croix-Rouge. Briefly, RBC units were gently mixed by inversion before collecting 5 mL of RCCs. After sample centrifugation at  $1,400 \times g$  for 10 min at 4°C, free Hb was measured using the Plasma/Low Hb System (HemoCue) while the total Hb content and the haematocrit (Hct) in non-centrifuged samples were measured with a haematological analyser (XN-10, Sysmex). Haemolysis was calculated by applying the following formula:  $\text{haemolysis} = (100\% - \text{Hct}\% \times \text{free Hb}) / \text{total Hb}$ .

## 2.8 | Determination of the three vesiculation cohorts

In order to identify the 'low', 'medium' and 'high' vesiculation cohorts, EV kinetics were presented for each RCC individually through colour associations and in the form of the precise storage days in Figure S1A. The three groups were defined based on the EV count at 42 days (the legal expiry date). Data distribution was then visualized using a Tukey box-plot (box-plot with whiskers corresponding to 1.5\*interquartile value; Figure S1B). The low vesiculation cohort was defined as the first quartile (Q1) corresponding to 25% of the dataset (area below the horizontal pink dotted line), the medium vesiculation cohort as the range from Q1 to the end of the upper whisker (area between the horizontal pink and grey dotted lines), since most of the data are concentrated in this area, and finally the high vesiculation cohort as the 'outliers' (data points that stand out from the upper whisker above the horizontal grey dotted line). The 'low' level contains RCCs with a vesiculation rate of 0–1.8 EVs/RBC (light green,  $n = 20$  RCCs), 'medium' level with a vesiculation rate of  $>1.8 - < 7.4$  EVs/RBC (intermediate green,  $n = 38$  RCCs) and 'high' level with a vesiculation rate of  $\geq 7.4$  EVs/RBC (dark green,  $n = 11$  RCCs). The entire cohort ( $n = 69$  RCCs) is represented by black symbols.

## 2.9 | Data presentation and statistical analysis

Kinetics during storage were represented in the form of weekly storage intervals (except in Figure S1). The end of the legal storage period is indicated by a vertical blue dotted line. When data from several RCCs were collected within the same storage week, the mean  $\pm$  SD was indicated in graphs. For the comparison of two time points, two vesiculation cohorts or two centrifugation protocols, an unpaired *t*-test (after logarithmic data transformation to fulfil normality and Welch's correction if needed) or a Mann–Whitney test was performed. Graphically, statistical significance is indicated above a horizontal full line connecting the two-time intervals. To compare the three vesiculation cohorts at 6w, the Kruskal–Wallis test with Dunn's multiple comparison was performed. For Spearman correlations, the coefficients (*r*) higher than 0.6 were plotted on the graphs as well as the associated slope (*s*) of the linear regressions.

# 3 | RESULTS

## 3.1 | Study design

Seventy RCCs were included in this study and followed over storage for different parameters. Due to limited supplies at Croix-Rouge, not all RCCs could be studied at all time points. Indeed, out of the 70 RCCs, 12 were delivered freshly (1 or 2 days of storage) to UCLouvain while six RCCs were provided at 1w, three RCCs at 2w, 17 RCCs at 3w, 20 RCCs at 4w, four RCCs at 5w and eight RCCs at 6w. Once received, their storage at 2°C–6°C was extended for up to 10w (Figure 1, Table S1). They corresponded to 68 donors as four RCCs originated from the same two donors and delivered at 1 or 2-years intervals. Moreover, among the 70 RCCs, one was only used for the comparison of particle measurement after sampling from a segment of the QC tubing or the mother-bag and was not studied for EV abundance. The internal code assigned to each RCC as well as the donor's characteristics are listed in the Table S1.

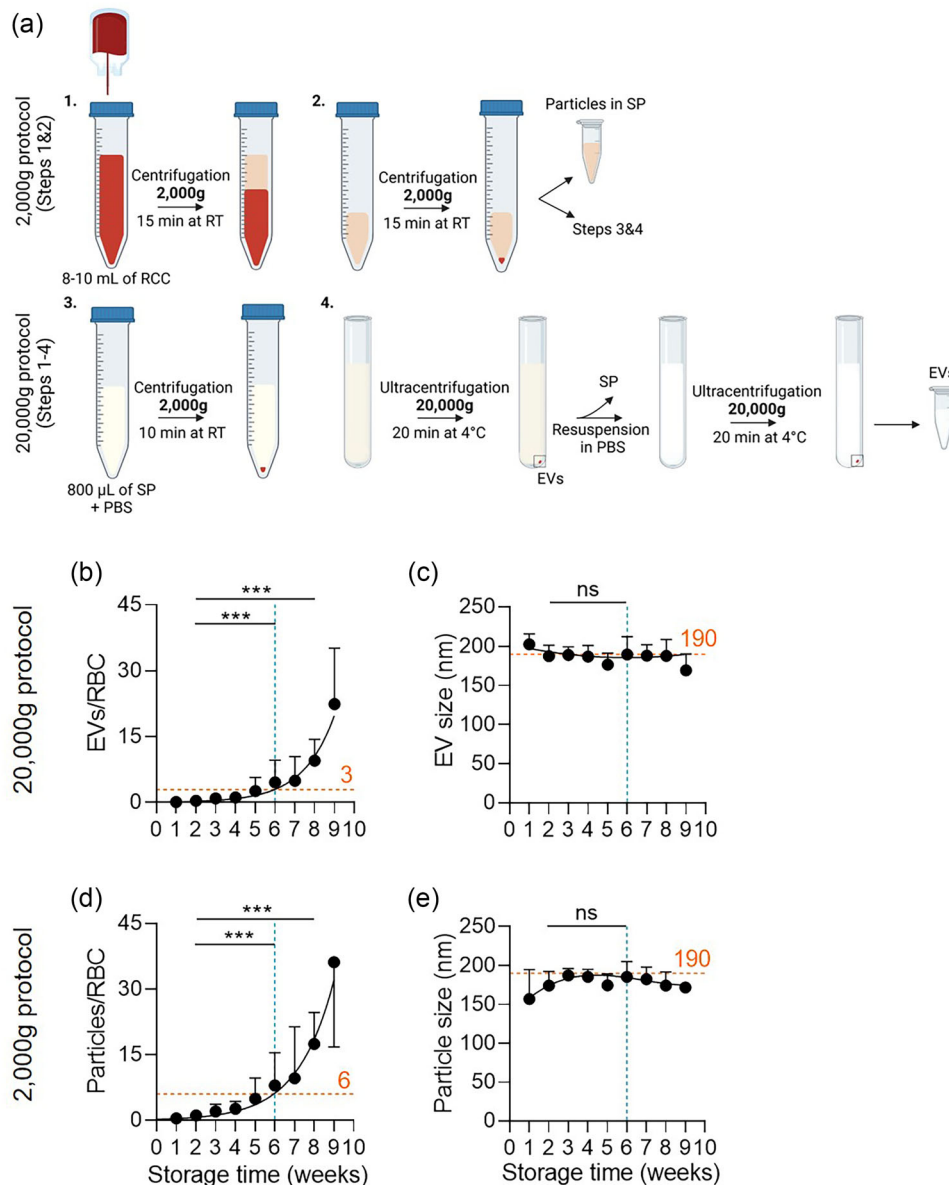


**FIGURE 2** The number of particles isolated with the  $2,000 \times g$  protocol increases exponentially during storage, similarly to EVs concentrated with the  $20,000 \times g$  protocol, but at a higher rate. (a) Schematic diagram of the  $2,000 \times g$  (steps 1 and 2) and  $20,000 \times g$  (steps 1 to 4) protocols. RBCs are first centrifuged at low speed at  $20^\circ\text{C}$  for 15 min to separate cells from the supernatant (SP, step 1). The recovered SP is centrifuged a second time using the same parameters (step 2) to remove the remaining cells. It is then either analysed directly (particles), or diluted in PBS and centrifuged as before for 10 min (step 3). The solution is next ultracentrifuged twice at  $4^\circ\text{C}$  to pellet extracellular vesicles (EVs; step 4). Created in BioRender. Ghodsi, M. (2025) <https://BioRender.com/q29x682>. (b,d) Number of EVs or particles determined by Nanoparticle Tracking Analysis (NTA) and expressed relative to the theoretical number of RBCs in RCCs. The mean number of EVs or particles at 6w is indicated by a horizontal orange dotted line. Unpaired t-test after logarithmic data transformation and when needed, Welch's correction. (c,e) Size of EVs or particles (in nm). The mean size throughout the storage period is indicated by a horizontal orange dotted line. Unpaired t-test. All data are expressed as mean  $\pm$  SD ( $n = 69$  RCCs). Statistical significance is indicated above a line connecting two time intervals. \*\*\*,  $p < 0.001$ ; ns, not significant. The maximum legal storage period of 6w is indicated by a vertical blue dotted line. For statistical analyses between protocols for EV and particle abundance and size at 1w, see Table S3.

### 3.2 | EVs and particles released in RCCs increase exponentially over storage but at different rates

In a previous publication, we developed a reproducible ultracentrifugation-based protocol to concentrate RBC-derived EVs. This protocol consists of separating SP from RBCs by two centrifugations at  $2,000 \times g$  for 15 min. Then,  $800 \mu\text{L}$  of SP are diluted in PBS and centrifuged at  $2,000 \times g$  for 10 min (Momen-Heravi et al., 2013). Finally, the solution is ultracentrifuged twice at  $20,000 \times g$  for 20 min ( $20,000 \times g$  protocol, steps 1–4, Figure 2a) (Ghodsi et al., 2023). We have here simplified this protocol by removing ultracentrifugation steps and directly analysing SP after step 2 ( $2,000 \times g$  protocol, steps 1,2, Figure 2a). We used the term 'particle'

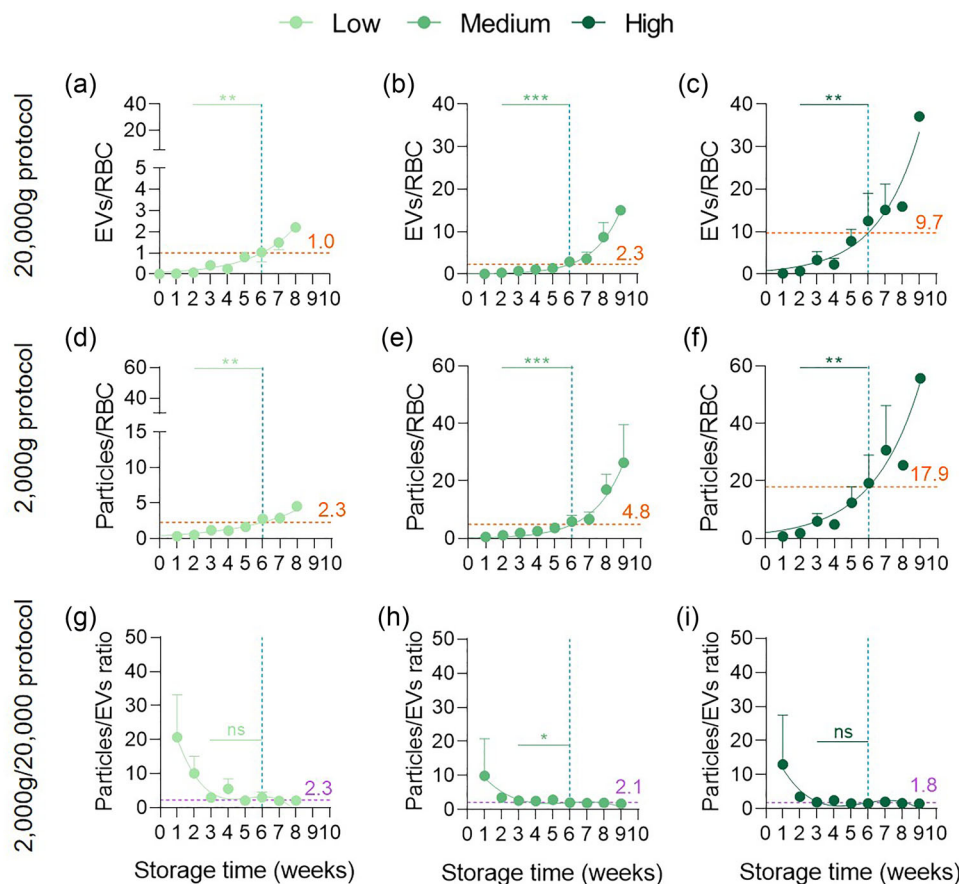


**FIGURE 3** The abundance of particles is  $\sim 2$ -fold higher than EV abundance from 3w of storage regardless of the vesiculation cohort. The 69 RCCs were classified into three groups based on their EV level at 42 days of storage. (a–f) Number of EVs (a–c) or particles (d–f) expressed relative to the theoretical number of RBCs in RCCs for each vesiculation group during storage. For a comparison of EV and particle size, see Figure S5. For statistical analyses, see Tables S2 and S3. (g–i) Ratio between the number of particles per RBC and the number of EVs per RBC at each time of storage. The mean number of EVs or particles and the mean particles-to-EVs ratio at 6w is indicated by a horizontal orange or purple dotted line on the graphs, respectively. All data are expressed as mean  $\pm$  SD. Mann–Whitney test. Statistical significance is indicated above a line connecting two time intervals. \*\*\*,  $p < 0.001$ ; \*\*,  $p < 0.01$ ; \*,  $p < 0.05$ ; ns, not significant. The maximum legal storage period of 6w is indicated by a vertical blue dotted line.

when EV identity was not confirmed or when contaminants were abundant in samples and the ‘EV’ generic term for material obtained with the  $20,000 \times g$  protocol (MISEV2023) (Welsh et al., 2024).

We started by comparing 69 RCCs for EV ( $20,000 \times g$  protocol) and particle ( $2,000 \times g$  protocol) abundance and size over storage. The number of both EVs and particles per RBC increased exponentially but quantitative differences were observed. At 6w, a mean of three EVs was obtained with the  $20,000 \times g$  protocol, while a mean of six particles was detected using the  $2,000 \times g$  protocol (Figure 2b,d). In contrast, the material size was similar at  $\sim 190$  nm in both protocols and quite stable between 2 and 6w but was reduced with the  $2,000 \times g$  compared with the  $20,000 \times g$  protocol at 1w (Figure 2c,e). Altogether, these data showed that the  $2,000 \times g$  protocol allowed for obtaining a higher particle yield than the  $20,000 \times g$  protocol.

### 3.3 | The particle-to-EV ratio stabilizes at $\sim 2$ from 3w to the end of storage in each vesiculation cohort

Using the  $20,000 \times g$  protocol, we previously evidenced a large variability in EV abundance between RCCs at 6w. This observation led us to classify them into three cohorts based on the EV level at this storage time (Ghodsi et al., 2023). This classification was also used in the present study but via the equations of the exponential curves of individual RCCs to estimate the number of EVs released at the legal expiry date of 42 days and thereby, to benefit from all RCCs, since EV measurements could not be performed at all time points (Figure S1A). Data distribution was then visualized using a Tukey box-plot. The ‘low’ rate was defined as  $0-1.8$  EVs/RBC, ‘medium’ rate as  $>1.8- < 7.4$  EVs/RBC and ‘high’ rate as  $\geq 7.4$  EVs/RBC (Figure S1B). The kinetics of the number of EVs/RBC were then plotted again in graphs for each cohort. As previously shown (Ghodsi et al., 2023), the curves were exponential with a significant increase between 2 and 6w and the amount of EVs released at 6w was significantly different between the 3 vesiculation cohorts (Figure 3a–c, Table S2). Consequently, we analysed whether RCC stratification was also valid



for particle measurement with the  $2,000 \times g$  protocol. Results were completely comparable (Figure 3d–f, Table S2) except for the rate of particle accumulation at 6w, which was still two-fold higher than the release of EVs, in the three vesiculation groups (Figure 3a–f) as it was for the entire RCC cohort (Figure 2b,d).

The significant difference between EV and particle levels in each vesiculation cohort did not result from a differential decrease in the number of RBCs during storage or donor variability due to the non-horizontal follow-up of RCCs. Indeed, we did not observe any decrease in the number of RBCs over time regardless of the vesiculation cohort, even after 6w of storage when haemolysis may exceed the legal threshold of 0.8% (Figure S2). Likewise, the kinetics of EVs and particles/RBC in six individual RCCs (two of each cohort) monitored throughout the whole storage period mirrored the curves of the corresponding overall cohorts (Figures S3 and 4).

Reassured by our RCC classification into cohorts, we then determined the evolution of the differential rate between EVs ( $20,000 \times g$  protocol) and particles ( $2,000 \times g$  protocol) throughout storage in all cohorts. We calculated a ratio between particles/RBC and EVs/RBC at all time points. In each cohort, we noticed a decreasing exponential curve characterized by a maximum ratio at 1w, oscillating in a similar way between vesiculation groups with  $\sim 15$ – $20$  times more particles than EVs (Figure 3g–i). The large standard deviations at this time suggested a high variability in the proportion of particles and/or EVs at the beginning of storage (Table S3). The difference in the particle-to-EVs ratio at 1w was also visible and significant for the entire cohort (Figure 2b,d and Table S3). Besides abundance, we also observed that the mean size of particles ( $2,000 \times g$ ) at 1w was lower in each vesiculation cohort compared with EVs ( $20,000 \times g$ ) and presented standard deviations systematically larger (Figure S5, Table S3), as for the entire cohort again (Figure 2c,e and Table S3). From 3w, the particle-to-EVs ratio stabilized at  $\sim 2$  (Figure 3g–i) and the material size remained stable at  $\sim 190$  nm until 6w (Figure S5, Table S2). A more in-depth analysis of the distribution of particle sizes of the 2 RCCs exhibiting the lowest mean size at 1w (Figure 2e) revealed a shift to the left compared with the distribution of sizes of EVs. This shift was considerably reduced but still visible at 7w (Figure S6A–D). Conversely, in the two RCCs with the highest mean particle size at 1w (Figure 2e), this shift was less visible at 1w and fully disappeared at 6w (Figure S6E–H). Thus, the lower mean size of particles at 1w observed in some RCCs can be linked to a more heterogeneous lower size distribution as compared to EVs.

Overall, these data indicated that particle abundance ( $2,000 \times g$  protocol) differed markedly between the three vesiculation cohorts, as did the abundance of EVs ( $20,000 \times g$  protocol). Additionally, although particle and EV numbers evolved similarly over time in the three groups, their rates differed, particularly at 1w of storage. Likewise, the size was statistically different between protocols at 1w and then stabilized at 190 nm. Altogether, these findings suggested that the material isolated with the  $2,000 \times g$  and  $20,000 \times g$  protocols could have a different composition.

### 3.4 | The $2,000 \times g$ protocol allows for the reproducible isolation of RBC-derived particles despite the presence of contaminants and can predict EV abundance

Our next goal was to assess whether the difference in materials obtained with the  $2,000 \times g$  and  $20,000 \times g$  protocols could result from a differential proportion of contaminants. Indeed, despite the removal of blood components during RCC preparation, a small amount of plasma (maximum 20 mL per RCC) remains in the final product (Bosman et al., 2008; Laurén et al., 2018), bringing potential contaminants (i.e. soluble proteins, lipoproteins, platelets (or their vesicles), and leucocytes (or their vesicles)). Since some of them are similar to EVs in density, structure and size (Nieuwland & Siljander, 2024), they can be co-isolated with RBC-derived EVs and may not be differentiated by NTA. We therefore characterized the  $2,000 \times g$  and  $20,000 \times g$  materials isolated from a low, medium, and high vesiculation RCC at 6w (to have sufficient material) with both protocols by Coomassie blue staining of proteins. RBC ghosts were loaded in increasing quantities in order to identify and estimate the proportion of material originating or not from RBCs (Figure 4a). The comparison of the two protocols indicated that, despite a relatively equivalent loaded protein content (Figure 4b), the relative proportion of the proteins was not similar (Figure 4a). For instance, five ‘non-RBC’ bands (grey arrows 1, 2, 4, 5 and 8) were detected in the  $2,000 \times g$  samples and only two (grey arrows 4 and 8) in the  $20,000 \times g$  samples (Figure 4a). To identify the origin of some of these bands, we performed Western blotting and looked for the presence of albumin (the major soluble plasma protein), lipoproteins through ApoB100 associated with VLDL/LDL and ApoA1 associated with HDL, platelets (or their vesicles) through CD41, and leucocytes (or their vesicles) through CD45. All of the above proteins were present in materials obtained with the  $2,000 \times g$  protocol but not with the  $20,000 \times g$  protocol, with the exception of albumin in small amounts and ApoB100 as traces, indicating the presence of contaminants in particle preparations (Figure 4a,d, low and highly exposed membranes in supplemental Figure S8). Moreover, the comparison of the band intensity in the  $2,000 \times g$  preparations with those in the plasma loaded in similar or three-fold higher quantities revealed that major contaminants in particle preparations were albumin and ApoB100, followed by ApoA1 (in the form of dimers (He et al., 2019)) and CD41 (appearing at lower molecular weight than expected, thus probably degraded), and then CD45 in trace amounts.

Besides the ‘non-RBC’ bands, the  $2,000 \times g$  and  $20,000 \times g$  preparations shared four (red arrows 3, 6, 7 and 10) and five (red arrows 3, 6, 7, 9 and 10) bands with RBC ghosts, respectively. Western blotting identified four proteins from three of these bands: (i) Band 3 (or anion exchanger 1; arrow 3), the most abundant integral protein of RBCs; (ii) flotillin-1, an integral membrane protein associated with EVs (arrow 6); (iii) GPA (or CD235a; arrow 6), a major integral protein of RBCs and a component of the

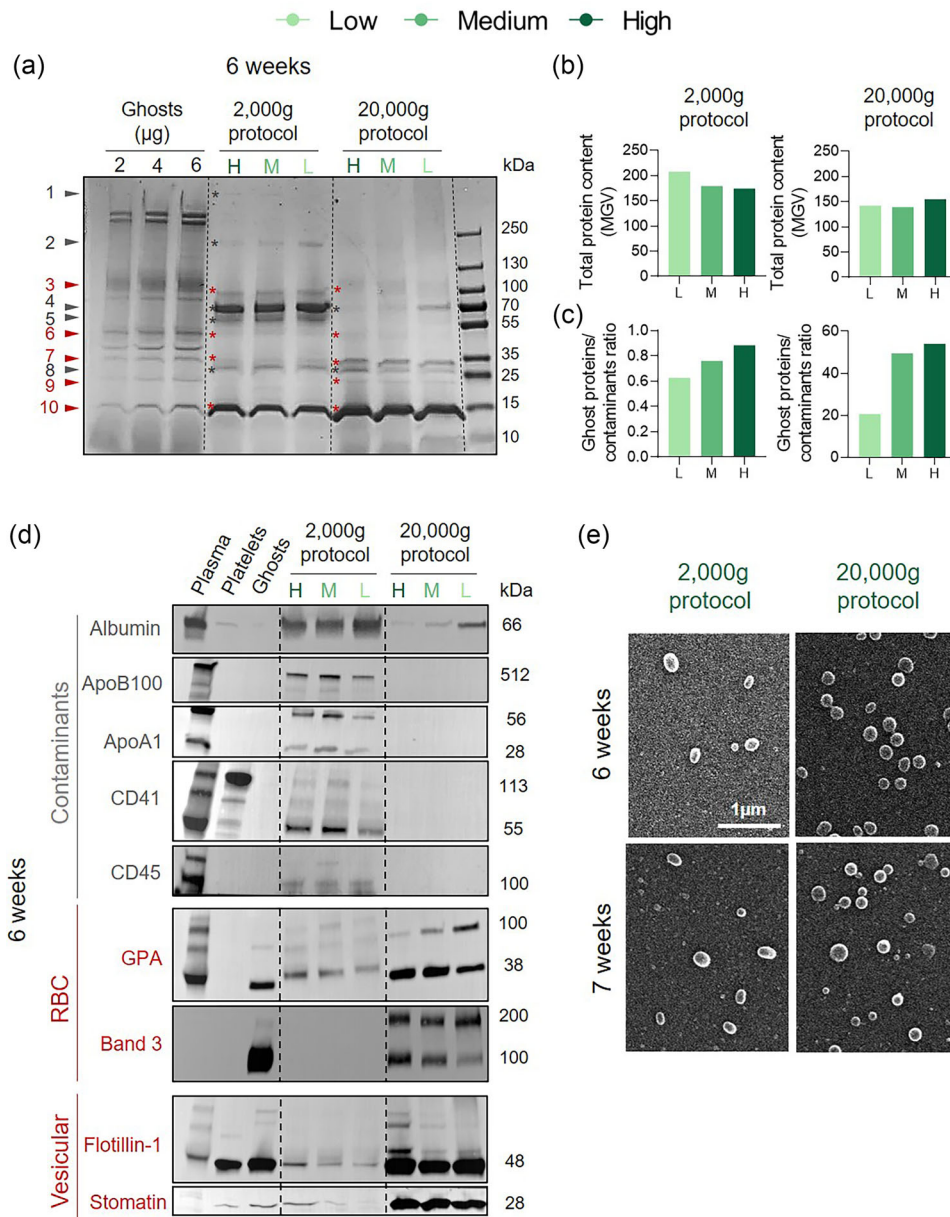


**FIGURE 4** The 2,000 × g protocol allows for recovering RBC-derived and vesicular material despite the presence of albumin, lipoproteins, platelet and leucocyte contaminants. (a–d) Characterization by Coomassie blue staining (a–c) and Western blotting (d) of 2,000 × g and 20,000 × g preparations obtained from high (H), medium (M) and low (L) vesiculation RCCs stored for 6w. (a) Coomassie blue stained gel for protein composition in 2,000 × g and 20,000 × g preparations. About 6 µg/well of EV and particle proteins were loaded. RBC ghosts (5 µL) and RBC ghosts were used as internal control and loaded in increasing quantities (2, 4 and 6 µg). (b) Total protein content calculated as the sum of all the bands (indicated by an asterisk in A) for each vesiculation cohort. (c) Ratio between the sum of MGV of proteins shared with RBC ghosts (red asterisk) and the sum of MGV of non-shared proteins (dark grey asterisk). (d) Western blots of albumin, lipoproteins (apolipoproteins B100 (ApoB100) and A1 (ApoA1)), platelet (CD41) and leucocyte (CD45) contaminants as well as RBC (glycophorin A (GPA) and Band 3) or vesicular (Flotillin-1 and stomatin) proteins. About 6 µg/well of EV and particle proteins were loaded. All proteins were revealed on individual membranes except ApoA1 and CD45 revealed on cut membranes. The molecular weight of monomers for each protein as well as of dimers for GPA, Band 3 and ApoA1 and of the lower band at 55 kDa for CD41 are indicated on the right. For non-cropped membranes, see Figures S8 and S9. Plasma (20 µg except for albumin membrane for which 6 µg were loaded) from blood tubes, platelet lysates (5 µL) and RBC ghosts (1 or 6 µg) were used as positive controls (see the table in Material and Methods section). Representative Western blots of 3–4 experiments for each protein (except for Band 3 and CD45, 1 experiment). (e) Morphology of 2,000 × g and 20,000 × g preparations isolated from a high vesiculation RCC stored at the indicated times, laid down on poly-L-lysine-coated coverslips and analysed by scanning electron microscopy (one experiment).

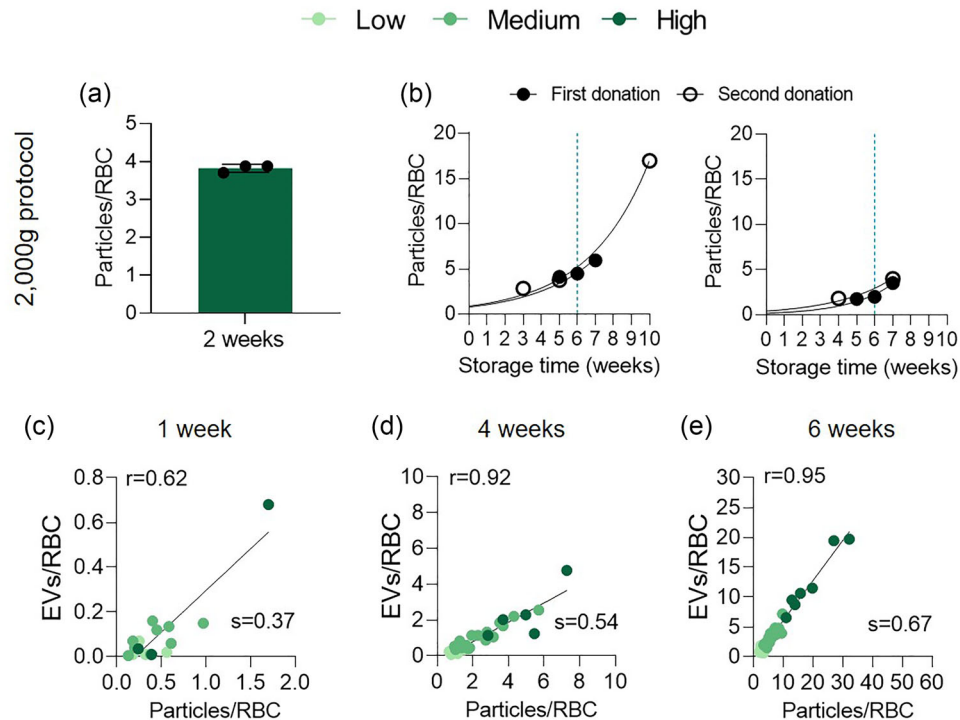


**FIGURE 5** The 2,000 × g protocol is reproducible and can be used to predict EV abundance. (a) Reproducibility of the 2,000 × g protocol. RBCs from 1 RCC of the high vesiculation cohort stored for 2w were sampled in triplicate. Next, particles were recovered with the 2,000 × g protocol and their abundance determined by NTA. Data are expressed as mean ± SD. (b) Kinetics of particle abundance in two RCC donations obtained at 1 or 2 years apart from the same donor (two different donors). The maximum legal storage period of 6w is indicated by a vertical blue dotted line. (c–e) Spearman correlations between particle and EV abundance at 1 (low,  $n = 4$ ; medium,  $n = 9$ ; high,  $n = 3$  RCCs), 4 (low,  $n = 6$ ; medium,  $n = 16$ ; high,  $n = 5$  RCCs) and 6w (low,  $n = 17$ ; medium,  $n = 28$ ; high,  $n = 7$  RCCs) of storage. Correlation coefficients ( $r$ ) and slopes ( $s$ ) of the linear regressions are plotted on the graphs.

ankyrin-1 complex appearing in the form of dimers (Auffray et al., 2001); and (iv) stomatin (or erythrocyte membrane protein band 7.2; arrow 7), an integral protein associated with EVs (Figure 4a,d). In 2,000 × g preparations, these different proteins were not (i.e. Band 3) or barely (i.e. flotillin-1, GPA and stomatin) detectable with a low exposition of the membranes but slightly visible with a higher exposition (Figure S9). The band at ~15 kDa (arrow 10) corresponded probably to Hb (Bolotta et al., 2018; Bosman et al., 2008). The presence of Band 3, Hb, GPA, and stomatin in EVs is consistent with previous studies on RCCs (leucoreduced or not) (Bosman et al., 2008; Kriebardis et al., 2008). The presence of vesicular material in both protocols was confirmed by electron microscopy (Figure 4e).

These data indicated that albumin and lipoproteins, besides their co-isolation due to their overlapping size range and density, seemed to outnumber RBC-derived EVs in the 2,000 g samples. Indeed, despite an increase in the abundance of material of interest in the high vesiculation RCCs, contaminants were in the majority at 6w. We therefore analysed the protein profile of the 2,000 × g and 20,000 × g preparations during storage. As observed above, contaminants in the 2,000 × g preparations were in greater abundance than RBC proteins throughout storage but decreased over time in favour of proteins of interest, reaching at 6w a ratio of ~1 at least in the medium and high vesiculation cohorts (Figure S7A,B). This observation was in accordance with the evolution of the ghost proteins-to-contaminant ratio over time in the 20,000 × g preparations, even if ultracentrifugation helped to highly concentrate RBC-derived EVs and get rid of almost all contaminants (Figure S7C,D).

Altogether, these data indicated that in 2,000 g preparations, contaminants were in significantly higher proportion compared to RBC-derived EVs, even at the end of storage. This is probably the origin of the very weak detection of some RBC proteins in 2,000 × g preparations by Western blotting. Nevertheless, the proportion of RBC-derived EVs over contaminants in the 2,000 × g preparations increased over storage and with the cohort vesiculation level (Figure 4c), exactly as in the 20,000 × g preparations.

One step further, we ensured that the presence of those contaminants in 2,000 × g preparations would not alter particle measurement reproducibility. As a consequence, we quantified particle number in triplicate of RBCs obtained from a high vesiculation RCC stored for 2w. We observed an identical number of particles/RBC (Figure 5a). We also analysed the particle abundance of four RCCs obtained at 1–2 years intervals from the same two donors (two RCCs per donor) during storage and evidenced a similar evolution (Figure 5b).

In summary, the 2,000 × g protocol was reproducible and allowed to recover RBC-derived EVs despite the presence of contaminants. Moreover, the positive correlations between particle and EV abundance became stronger as storage progressed (i.e. 1, 4 and 6w, Figure 5c–e), suggesting that particle number could predict EV number, at least reliably after 1w.

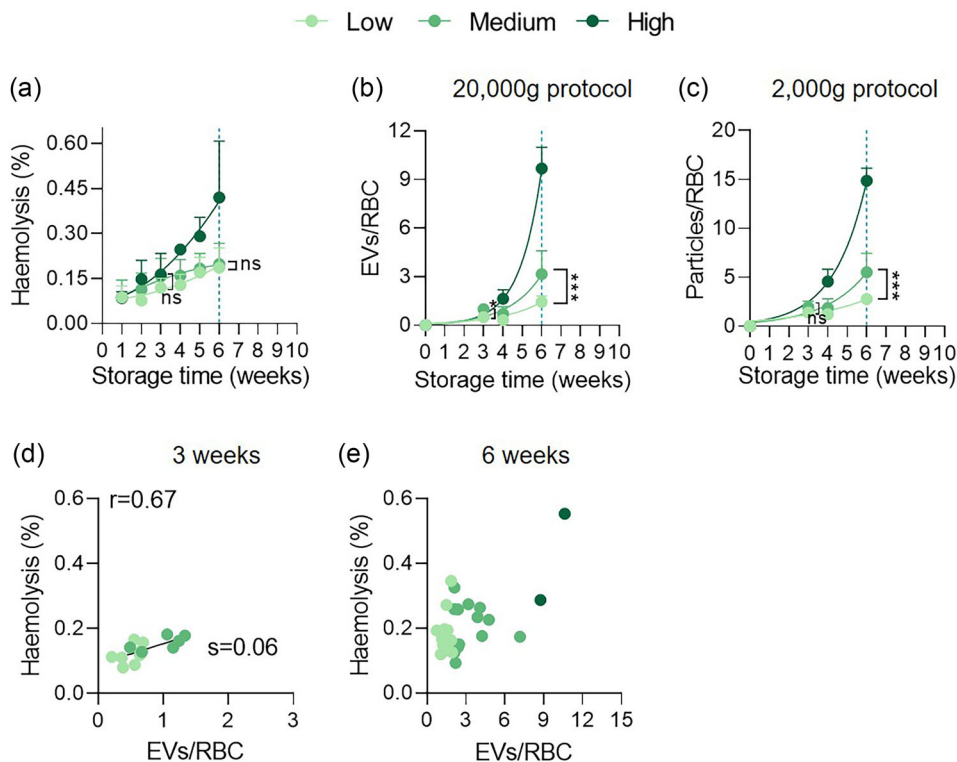


**FIGURE 6** Particle abundance allows for a better discrimination between the low and medium vesiculation cohorts than haemolysis at the legal storage expiry date. Comparison of the three vesiculation cohorts (low,  $n = 12$ ; medium,  $n = 15$ ; high,  $n = 2$  RCCs) during storage for the percentage of haemolysis (a) and EV (b) or particle (c) abundance. The maximum legal storage period of 6w is indicated by a vertical blue dotted line. (a) Haemolysis was determined by the measurement of free Hb using the Plasma/Low Hb system after sample centrifugation, and the total Hb content and the haematocrit (Hct) in non-centrifuged samples on a haematological analyser. Haemolysis was calculated using the following formula:  $(100 - \text{Hct} \% \times \text{free Hb}) / \text{total Hb}$ . Unpaired  $t$ -test after logarithmic transformation of data from the low and medium vesiculation cohorts at 3 and 6w of storage. (b,c) EVs and particles were recovered from 10 mL of RCCs with the  $20,000 \times g$  protocol and the  $2,000 \times g$  protocol, respectively. Then, their abundance per RBC was determined per NTA. Mann-Whitney test. All data are expressed as mean  $\pm$  SD. Statistical significance at 3 or 6w between the low and the medium vesiculation cohorts is indicated next to a curly bracket. Statistical analysis could not be performed on the high vesiculation cohort ( $n = 2$  RCCs). \*\*\*,  $p < 0.001$ ; \*,  $p < 0.05$ ; ns, not significant. (d,e) Spearman correlations between haemolysis and EV abundance at 3 (low,  $n = 8$ ; medium,  $n = 6$  RCCs) and 6w (low,  $n = 12$ ; medium,  $n = 15$ ; high,  $n = 2$  RCCs) of storage. In (e), the correlation coefficient ( $r$ ) was  $< 0.6$  and therefore not plotted on the graph.

### 3.5 | Particle and EV abundance discriminate better between medium and low vesiculation cohorts than haemolysis at 6w of storage

We then compared 29 RCCs for the extent of EV and particle release with haemolysis, analysed in routine at the legal expiry date. Haemolysis measurements were performed on the 29 RCCs at each storage time while EV and particle count could be performed at only two time points (3 or 4 and 6 weeks). As expected, haemolysis was under the regulated limit of 0.8% for the 29 RCCs (Figure 6a). However, its extent was higher in the high vesiculation cohort as compared with the two other cohorts. A similar observation was obtained for EV and particle release (Figure 6b,c). Regarding the low and medium vesiculation cohorts, they showed a similar increase in haemolysis over time and could not be statistically discriminated even at the end of the legal storage period, in contrast to EV and particle kinetics (Figure 6a–c). Accordingly, although both increased exponentially during storage, EV abundance and haemolysis showed weaker correlations compared with those between EV and particle abundance at similar time points (Figures 5 and 6d,e). Overall, these data suggested that particle measurement could represent an interesting parameter to better discriminate RCCs, particularly at 6w.

### 3.6 | The relative centrifugal force can be adapted to a small RCC volume to obtain similar particle abundance as in a large volume

At Croix-Rouge, QC parameters are routinely performed on RBCs collected from a segment of the QC sampling tubing attached to RCC. The maximal volume in the whole tubing is approximately 2 mL. Consequently, to implement particle measurement during RCC validation and QC, it requires their concentration from smaller sample volumes (ideally 0.5 mL to leave sufficient volume for other analyses) than those so far (8–10 mL). A consequence is that the relative centrifugal force (RCF) applied to RCC

samples has to be adapted to avoid modification of the material sedimentation and the particle yield. Indeed, the RCF depends in part on the distance of the sample from the rotational axis (the greater the distance, the greater the  $g$ -force) (Sharifian Gh & Norouzi, 2023).

To determine how the particle yield could be affected in 0.5 mL samples, we compared the particle abundance in four different RCC volumes from one high vesiculation RCC stored for 3w. We observed a gradual reduction of particle number (Figure 7a). Since there are no existing equations to adapt centrifugation parameters to the sample volume, we modified the centrifugation time. Four samples of 0.5 mL were collected, centrifuged twice at  $2,000 \times g$  for 20, 15, 10 or 5 min and compared with a sample of 10 mL centrifuged with the usual parameters ( $2,000 \times g$  for 15 min). The number of particles per RBC in the SP increased progressively when the centrifugation time decreased but it never reached the level of particles per RBC found in the 10 mL sample (Figure 7b, dotted line). We then calculated a ratio (10 mL/0.5 mL) of particles/RBC for the four different conditions and plotted these ratios as a function of RCF  $\times$  time applied on the samples (Figure 7c).

Using the equation of the linear regression, we could determine the RCF  $\times$  time ( $4760 \times g \times \text{min}$ ) needed to have a ratio of 1, meaning no difference in the number of particles between 0.5 and 10 mL. Accordingly, 10 and 0.5 mL of RBCs at 4w from the above RCC were centrifuged at  $2,000 \times g$  for 15 min ( $2,000 \times g$  protocol, Figure 2a) and  $1,000 \times g$  for 5 min ( $1,000 \times g$  protocol, Figure 7d), respectively, allowing for obtaining an identical amount of particle/RBC (Figure 7e). Similar results were observed on one RCC from the medium vesiculation group (Figure S10). These data indicated that reducing RCC volumes has an impact on particle yield. However, this can be overcome by adapting centrifugation parameters (time and RCF).

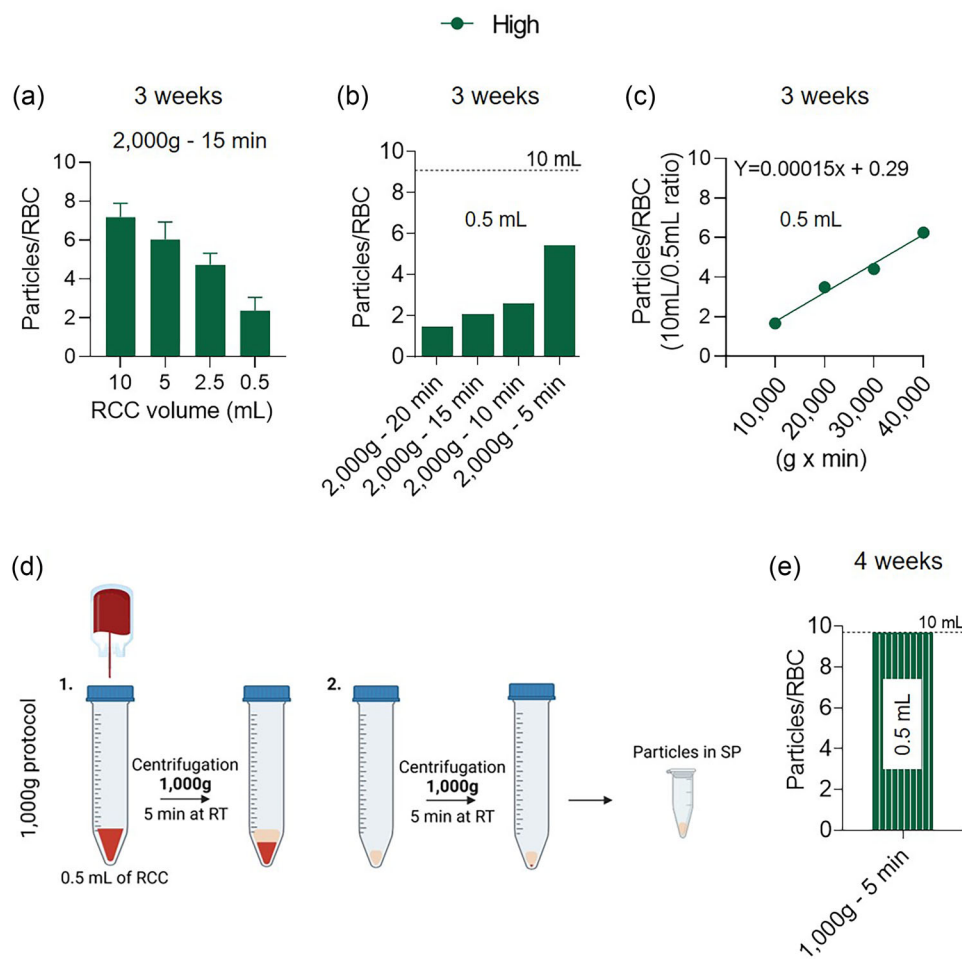


**FIGURE 7** Particle abundance is identical in small and large volumes of RCCs once centrifugation parameters are adapted. Comparison of particle abundance obtained from a high vesiculation unit at 3 and 4w of storage after centrifugation of variable volumes of RCC or for different timings and/or RCFs. For data on a medium vesiculation RCC, see Figure S10. (a) Comparison of the particle number obtained from the indicated RCC volumes with the  $2,000 \times g$  protocol. Data are expressed as mean  $\pm$  SD of two experiments in the same storage week. (b) Comparison of the particle number obtained from three samples of 0.5 mL centrifuged twice at  $2,000 \times g$  for the indicated centrifugation timings and compared with a sample of 10 mL centrifuged with the usual parameters ( $2,000 \times g$  for 15 min; dotted line) (one experiment). (c) Ratio between the number of particles in 10 mL of RCC and the three samples of 0.5 mL as a function of the centrifugation parameters expressed in  $g \times \text{min}$ . The equation of the linear regression is plotted on the graph. (d) Schematic diagram of the  $1,000 \times g$  protocol. 0.5 mL of RCC are centrifuged at  $1,000 \times g$  at  $20^\circ\text{C}$  for 5 min to separate cells from the SP. Recovered SP is centrifuged a second time using the same parameters to remove any remaining cells and then directly analysed. Created in BioRender. Ghodsi, M. (2025). <https://BioRender.com/v27b306>. (e) Comparison of the particle number obtained with the  $1,000 \times g$  protocol from 0.5 mL of RCC and with the  $2,000 \times g$  protocol from 10 mL of RCC (dotted line).

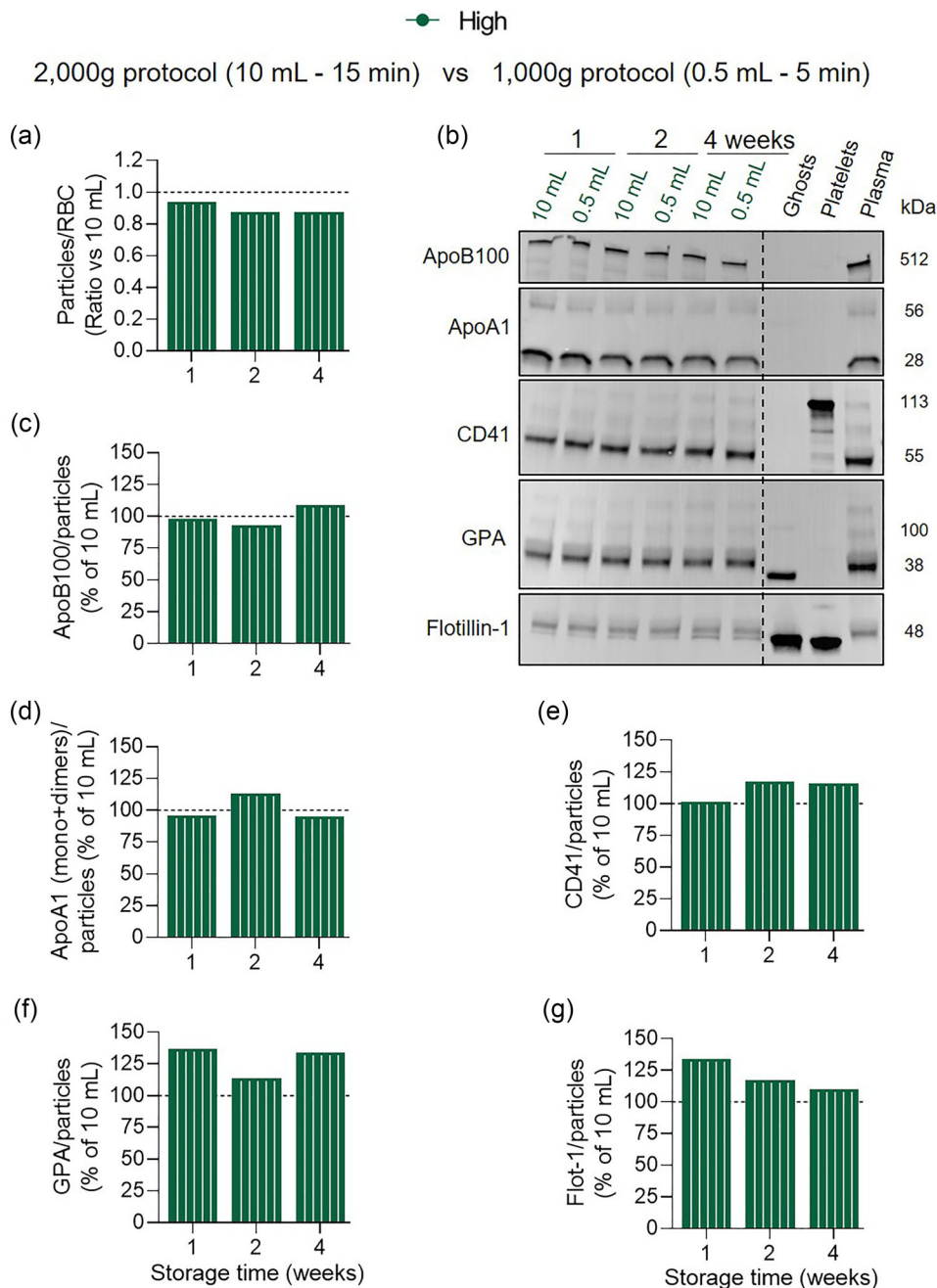


**FIGURE 8** Adapting the RCF and time of the 1,000 × g protocol for small RCC volumes results in a protein composition similar to that in large RCC volumes with the 2,000 g protocol. Comparison of the material composition recovered with the 2,000 g protocol from 10 mL of a high vesiculation RCC (dotted lines) and with the 1,000 × g protocol from 0.5 mL at the indicated storage times. (a) Ratio between the number of particles in 0.5 mL and 10 mL of RCC. (b-g) Western blots for lipoprotein (ApoB100 and ApoA1) and platelet (CD41) contaminants as well as for the presence of RBC (GPA) and vesicular (Flotillin-1) markers. 6 µg/well of particle proteins were loaded. All proteins were revealed on individual membranes except ApoA1, which was revealed after GPA membrane stripping. Plasma (6 µg), platelet lysates (5 µL) and RBC ghosts (1 µg) were used as positive controls. (c-g) Quantitative analysis of protein abundance in particle preparations. MGVs were normalized by the number of particles in the gel. Then, values obtained for 0.5 mL of RCC were expressed as a percentage of 10 mL of RCC at the corresponding storage time. Representative of 2–3 experiments for each protein.

### 3.7 | Adaptation of centrifugation parameters on a small RCC volume allows for obtaining similar particle protein composition as in a large volume with the 2,000 × g protocol

We then asked whether the similar number of particles between the 1,000 × g protocol used on 0.5 mL of RBCs and the 2,000 × g protocol used on 10 mL (Figure 7e) was also reflected in protein composition. To answer this question, particles of a high vesiculation RCC stored for 1, 2 or 4w were prepared from 0.5 or 10 mL of RBCs with adapted centrifugation parameters and compared for

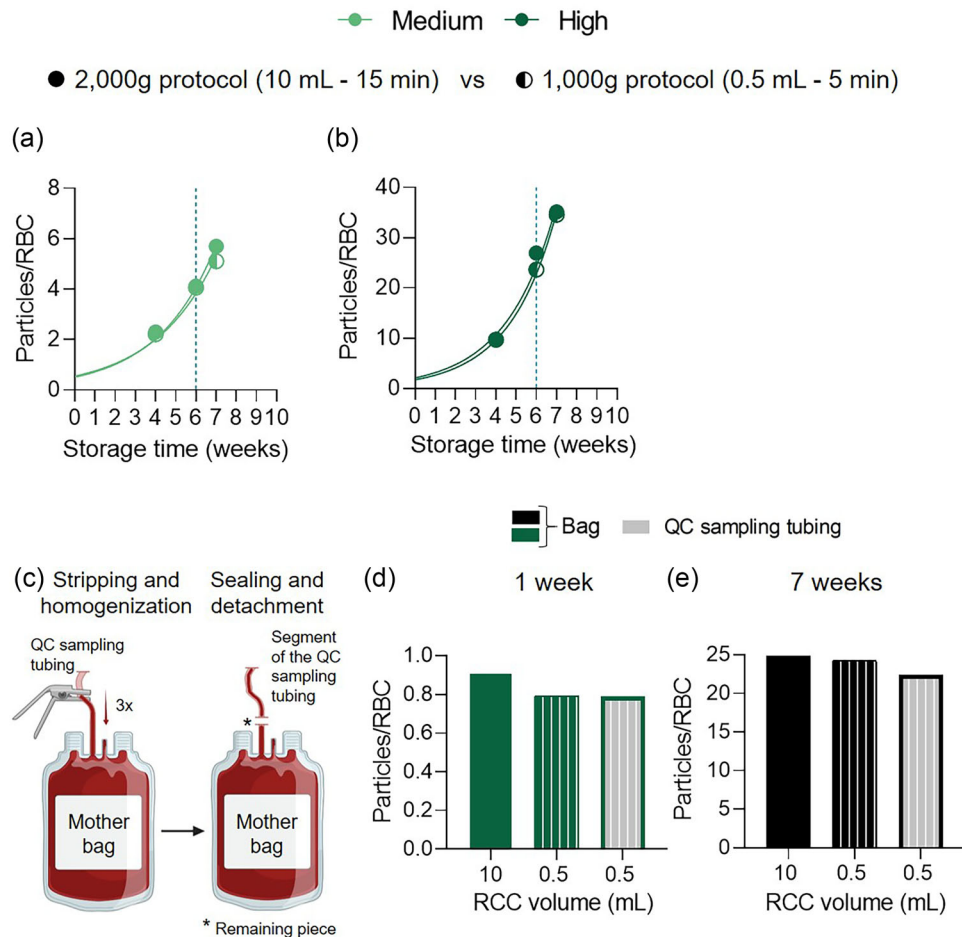


**FIGURE 9** The protocol adapted for small RCC volumes is suitable regardless of the storage time, vesiculation cohort or the sampling from a segment of the QC tubing or the mother-bag. (a,b) Comparison of the particle abundance obtained with the 1,000 × g protocol from 0.5 mL of RCC (half-filled symbols) and with the 2,000 × g protocol from 10 mL of RCC (filled symbols) at the indicated times from a medium (a) and a high (b) vesiculation RCC. The abundance of particles was assessed by NTA and expressed per RBC. The maximum legal storage period of 6w is indicated by a vertical blue dotted line. See Figure S11 for similar data on three other RCCs. (c) Schematic representation of the stripping, homogenization, sealing and detachment steps of a segment of the QC sampling tubing from a RCC. Created in BioRender. Ghodsi, M. (2025) <https://BioRender.com/137j485>. (d,e) The content of the QC sampling tubing from two RCCs stored for 1 and 7w was homogenised three times with the main unit. One segment was sealed, detached and opened to collect 0.5 mL (striped grey columns). Then, the QC sampling tubing was opened to have direct access to the inside of the mother-bag and to recover 10 mL or 0.5 mL (filled and striped green columns, respectively). 0.5 mL of RCC were centrifuged with the 1,000 × g protocol while 10 mL were centrifuged with the 2,000 × g protocol. Particle number was then measured in each condition.

abundance (Figure 8a) and protein composition (Figure 8b–g). The amount of particles/RBC, contaminants (ApoB100, ApoA1, CD41) and proteins of interest (GPA and flotillin-1) was similar between the small and large RCC volumes at each storage time. In conclusion, the 1,000 × g protocol for small volumes allowed for obtaining similar particle yield and composition.

### 3.8 | Adapted centrifugation parameters on a small RCC volume allow for obtaining similar particle abundance along storage time

To next determine whether the above observations could be confirmed on several RCCs of different vesiculation cohorts over the whole storage period, five RCCs were analysed. 0.5 or 10 mL of RBCs were collected and centrifuged with the 1,000 × g or 2,000 × g protocols, respectively. Regardless of the RCC and the storage time, the adaptations of centrifugation parameters for the small RCC volume (0.5 mL) allowed for obtaining similar particle counts as in 10 mL (Figure 9a,b, Figure S11). These data suggested that this protocol is suitable for particle recovery starting from 0.5 mL of RBCs.

### 3.9 | Particle number in the QC sampling tubing is representative of the particle number in the mother-bag

For routine tests, a rapid and non-destructive method is needed. Therefore, we assessed on two RCCs (one of the high vesiculation cohort and one for which EV number was not determined) stored for 1 or 7 weeks, respectively, whether the particle measurement is possible on the QC sampling tubing and more importantly whether it is representative of the mother-bag. The content of the QC tubing was stripped, and homogenized three times with the main unit. Then, to maintain RCC integrity, a segment of the tubing was sealed, detached and opened to collect 0.5 mL (Figure 9c). For the comparison with the bag, the remaining piece of QC sampling tubing was opened to recover 10 mL or 0.5 mL. Once again, small volumes were centrifuged two times at  $1,000 \times g$  for 5 min while the larger volume was centrifuged twice at  $2,000 \times g$  for 15 min. As previously, the particle abundance in 0.5 mL from the mother-bag was similar to that in 10 mL for both RCCs. It was also the case between 0.5 mL from the segment of the QC sampling tubing and the main bag (Figure 9d,e). Consequently, this simple and fast protocol was appropriate for particle measurement and ensured RCC integrity.

## 4 | DISCUSSION

### 4.1 | Main observations

In order to develop an easy-to-use method for routine EV measurement, we first compared a previously validated ultracentrifugation-based protocol ( $20,000 \times g$ ) (Ghodsi et al., 2023) with a simpler one ( $2,000 \times g$ ). A difference in the material yield was evidenced between the two protocols and was mainly attributed to a greater proportion of contaminants in the  $2,000 \times g$  preparations. To fit with routine requirements, several adaptations of the  $2,000 \times g$  protocol were made such as modification of the centrifugation time and g-force ( $1,000 \times g$  protocol) to recover the same material yield and composition in small RCC volumes compared to larger volumes. Even if  $2,000 \times g$  preparations were less pure, particle number (i) was reproducible between triplicates and different RCC donations from the same donor, (ii) could predict the EV number obtained with the  $20,000 \times g$  protocol, (iii) better discriminated between vesiculation cohorts than haemolysis at the legal expiry date, and (iv) was similar between the QC sampling tubing and the mother-bag. The latter observation validated the measurement as a non-destructive method. Altogether, these data suggested that particle measurement with the  $2,000 \times g$  protocol (adapted to  $1,000 \times g$  protocol) could represent a good additional parameter to be included in the routine procedure.

### 4.2 | The centrifugation parameters affect the yield and composition of EV and particle preparations

As previously shown by our group and others, the EV number increases exponentially during storage (Almizraq et al., 2017; Ghodsi et al., 2023; Laurén et al., 2018; Rubin et al., 2008). However, the absolute number varies largely between studies mainly due to blood manufacturing methods, storage conditions as well as EV isolation and detection techniques (Almizraq et al., 2017, 2018; Gamonet et al., 2020). In the present study, we excluded any variability in RCC processing and storage conditions since: (i) RCCs were all prepared at Croix-Rouge, (ii) RCCs were stored identically at Croix-Rouge and at UCLouvain (between  $2^\circ\text{C}$  and  $6^\circ\text{C}$  without agitation), and (iii) the four RCCs obtained from the same two donors, 1 or 2 years apart, showed identical exponential curves for EV (Ghodsi et al., 2023) and particle abundance whereas delivery at UCLouvain and measurements were carried out at different storage times.

Different EV isolation methods have been described and the choice of the technique has been shown to greatly impact EV yield and purity (Brennan et al., 2020; Takov et al., 2018; Zimmerman et al., 2024). Until now, no method has been able to isolate EVs from RCCs without the presence of contaminants. In final RCCs, a maximum of  $\sim 20$  mL of plasma persists (Bosman et al., 2008; Laurén et al., 2018), bringing soluble proteins, lipoproteins as well as platelets, and leucocytes (or their vesicles). Most of them have similar structure, size and density as EVs (Théry et al., 2018; Welsh et al., 2024). Therefore, it is challenging to separate them from each other (Stam et al., 2021). Nevertheless, some isolation methods can be more powerful than others to minimize them. For example, Takov et al. (2018) showed that, whereas ultracentrifugation induces a reduced EV yield, it provides higher purity with lower ApoB and non-EV protein contaminations compared with conventional size-exclusion chromatography. Furthermore, even using the same technique, substantial variability can be found, notably because of the varying steps between protocols. In the field of RBCs, differential (ultra)centrifugation is the gold standard approach to concentrate RBC-derived EVs. However, protocols can consist of one or two steps of low-speed centrifugation with a wide range of RCFs and times ( $600\text{--}3000 \times g$  for 10–20 min). Volumes of RCC engaged are usually  $\sim 10\text{--}15$  mL of RBCs but not always specified, and are sometimes pre-diluted in PBS (Almizraq et al., 2018; Gamonet et al., 2017; Hashemi Tayer et al., 2019; Laurén et al., 2018; Momen-Heravi et al., 2013).



Moreover, low-speed centrifugations can be followed or not by a double ultracentrifugation characterized by different RCFs and times ( $16,000\text{--}20,000 \times g$  for 20–30 min) to pellet EVs (Cloos et al., 2020; Tripisciano et al., 2020). Altogether, a high diversity of protocols exists, but the steps are rarely justified and sample composition is not always characterized, preventing comparison between studies.

By comparing the  $2,000 \times g$  and  $20,000 \times g$  protocols, we observed that material yield was significantly different regardless of the storage time. This can be explained by the following hypotheses. First, this difference could be attributed to the reduction of contaminants in the  $20,000 \times g$  preparations (Brennan et al., 2020; Takov et al., 2018), as observed in Western blots and Coomassie blue stained gels. Indeed, the duration of sedimentation of a dispersed sample is proportional to the viscosity and the pathlength of a suspension as well as inversely proportional to the average diameter of a dispersion (e.g. EVs, lipoproteins) and the difference in densities between the dispersion and the solvent (Sharifian Gh & Norouzi, 2023). This means that the introduction of PBS at step 7 of the  $20,000 \times g$  protocol changed the viscosity of the medium as well as the final volume in the tube (distance of EVs or particles from the rotational axis). Due to their smaller size compared with RBC-derived EVs, albumin (which can form aggregates of  $\sim 100$  nm (McNicholas et al., 2017)) and lipoproteins (VLDL 30–80 nm, LDL 18–25 nm and HDL 5–12 nm (Wasan et al., 2008)), major contaminants in this study, will need higher RCF for longer periods (i.e.  $100,000 \times g$  for 24 h) to be concentrated (Li et al., 2018). This could also be true for other unexamined contaminants such as RBC waste products accumulating during storage (Yoshida et al., 2019). Besides size, RBC-derived EVs and lipoproteins could also differ in density. By accumulating Hb during storage, RBC-derived EVs could become denser and be pelleted more rapidly (Bosman et al., 2008; Tzounakas et al., 2022). Second, part of the material of interest could have been lost in  $20,000 \times g$  preparations due to the multiplication of steps including washes and resuspensions of the EV pellet (Brennan et al., 2020). The difference in the proportion of contaminants and material of interest introduced between the 2 protocols could explain why RBC proteins (Band 3, flotillin-1, GPA and stomatin) were not as well detectable in the  $2,000 \times g$  as in the  $20,000 \times g$  preparations by Western blotting, even though part of the SP obtained with the  $2,000 \times g$  protocol was used to concentrate EVs. Since the material in the  $2,000 \times g$  samples was less concentrated and contained more contaminants, loading similar protein content into the Western blots for the  $2,000 \times g$  and  $20,000 \times g$  samples did not result in a similar abundance of EVs. Therefore, longer membrane exposure times were needed to reveal the proteins of interest.

We also showed that modifying centrifugation time (5, 10, 15, 20 min) for a similar RCC volume and RCF or RCC volumes (10 vs. 0.5 mL) for a similar time and RCF can also affect particle yield. By increasing only the centrifugation time, the RCF applied on the sample lasts for a longer time, resulting in the sedimentation of a greater number of particles, and thus reducing the yield in the SP. By reducing only the volumes (0.5 vs. 10 mL), the length of the particle sedimentation path is reduced, which again results in the sedimentation of a greater number of particles. We could have observed the same results by modifying the RCF or the rotor. Indeed, Rubin et al. (2008) reported that the abundance of particles isolated from a stored RCC decreases with increasing RCF. Regarding the effect of the rotor, Cvjetkovic et al. (2014) compared the exosomal yield from human mast cells after centrifugation with a fixed-angle or swinging rotor and revealed that applying the same RCF  $\times$  time was not sufficient to obtain similar protein and RNA content in exosome preparations (Cvjetkovic et al., 2014). Indeed, different rotors have different radii and therefore different sedimentation pathlengths. Additionally, for the same rotor, RCF will not be identical all along the sample. A particle close to the bottom of the tube will undergo a greater RCF during sedimentation and be pelleted before complete sedimentation (Sharifian Gh & Norouzi, 2023).

### 4.3 | NTA detects both RBC-derived EVs and major contaminants but lacks precision regarding size measurement

The detection method can also impact the absolute number of EVs or particles. Laurén et al. (2018) reported by NTA that the number of EVs climbs up to  $\sim 10^7$  EVs/ $\mu\text{L}$  after 42 days of storage, which is in concordance with our results. Nevertheless, other groups using flow cytometry-based approaches reported considerably lower numbers, between 650 and 20,000 RBC-derived EVs/ $\mu\text{L}$  after 42 days (Almizraq et al., 2017; Gamonet et al., 2020; Roussel et al., 2017; Rubin et al., 2008). This difference is at least partly due to the differential sensitivity and specificity of the techniques. Conventional flow cytometry-based approaches are more specific but have difficulty detecting particles smaller than 300 nm (Serrano-Pertierra et al., 2020). Moreover, by using only certain markers (mostly GPA, CD47 and phosphatidylserine) to discriminate cell origin, they could not reflect all EV subpopulations and therefore underestimate the total amount. In contrast, techniques such as NTA or tuneable resistive pulse sensing (TRPS) have better sensitivity but are not specific since they are based on light diffraction or transient changes in the ionic current flow, respectively (Dlugolecka et al., 2021). Therefore, they probably overestimate EV abundance (Stam et al., 2021) and do not differentiate EVs of interest from co-isolated contaminants including large lipoproteins (chylomicrons and VLDL) and albumin aggregates (McNicholas et al., 2017; Nieuwland & Siljander, 2024; Stam et al., 2021). Nevertheless, we showed here that the measurement of particles ( $2,000 \times g$  protocol) was reproducible and that the difference in abundance between particles and EVs was stable from 3w in each vesiculation cohort. This could explain why the classification of RCCs into cohorts was still valid with

this protocol. Finally, the evolution of material of interest compared to contaminants in  $2,000 \times g$  samples increased over time, exactly as the material isolated with the  $20,000 \times g$  protocol.

Contaminants in the form of lipoproteins and albumin were in the majority in particle samples compared to EV samples throughout the storage period. Therefore, the similar size of  $\sim 190$  nm between particles and EVs from 2 to 6w of storage was surprising but could be explained by two hypotheses. First, NTA has difficulty distinguishing particles differing in size by less than 1.5 times (van der Pol et al., 2013) and it is more sensitive to larger particles in a heterogeneous preparation (Bachurski et al., 2019; Kashkanova et al., 2023). Indeed, Kashkanova et al. (2023) observed that the distribution of sizes for melanoma EVs and commercial lipoproteins solutions by NTA is larger and shifts towards a greater size compared to interferometric NTA. Second, the presence and accumulation of contaminant aggregates and their potential adherence to RBC-derived EVs could distort the mean size. The surface of RBC-derived EVs isolated during storage was shown to be covered by particles of 5–15 nm in diameter, presumably membrane proteins or protein aggregates (Bebesi et al., 2022). However, despite the above limitations, our measurements were in concordance with other studies (Almizraq et al., 2017; Bebesi et al., 2022; Bicalho et al., 2016). For example, Almizraq et al. (2017) reported an increase in EV size between 1 and 2w with a stabilization at  $\sim 200$  nm from 2w to the end of storage. They used a similar isolation protocol of differential centrifugation at low speed ( $2,000 \times g$  for 15 min) and detection technique (dynamic light scattering, DLS) (Almizraq et al., 2017).

Altogether, these data suggested that despite size limitations, NTA could detect both RBC-derived EVs and contaminants, at least the major ones highlighted by Coomassie blue and Western blotting in the  $2,000 \times g$  protocol (albumin and ApoB100). The lack of precision in size measurements does not represent an important issue for the applicability of the  $2,000 \times g$  protocol in routine use.

#### 4.4 | Particle abundance measurement could anticipate the extent of vesiculation in RCCs during storage

Several lines of evidence provided in this study suggest that particle isolation via the  $2,000 \times g$  protocol could be relevant for predicting the extent of vesiculation in RCCs. First, even though  $2,000 \times g$  preparations were less pure than  $20,000 \times g$  preparations, the particle number was reproducible between triplicates and different RCC donations from the same donor. Second, EV and particle abundance strongly correlated during storage. Third, similar particle abundance was obtained between the QC sampling tubing and the mother-bag, validating the measurement as a non-destructive method. Fourth, the classification in three cohorts based on the EV level at 42 days of storage was still valid for the material isolated at  $2,000 \times g$ . We investigated for an effect of the donor's characteristics to explain the variability between RCCs within a specific storage interval. However, within our specific cohort of 69 RCCs, no statistical differences were found. Only trends could be observed: EV abundance tended to increase in men, in donors over 50 years, and in AB blood group donors (data not shown). This is generally consistent with the study of Gamonet et al., including 264 RCCs, which also showed no significant differences in EV abundance according to donor sex or age but described higher EV levels in RCCs from donors with the blood group B and with higher RBC counts (Gamonet et al., 2020). Nevertheless, other unexplored parameters could be implicated and remain to be studied such as BMI, genetic profiles, ethnicity, smoking status... (Hadjesfandiari et al., 2021).

#### 4.5 | Particle abundance measurement could represent a new quality biomarker in addition to haemolysis

Blood centres are increasingly interested in implementing new parameters to assess RCC quality in routine (Acker et al., 2018; Klei et al., 2023). Indeed, the only well-established quality parameter used nowadays to reflect storage lesions is haemolysis. However, although easy and inexpensive, the haemolysis rate is very low and only informative at the end of storage. Moreover, haemolysis is determined by measuring free Hb in the SP but most optical methods do not distinguish residual RBCs and Hb-enclosed EVs from free Hb (Acker et al., 2018). Protocols for this measurement usually consist of a low-speed centrifugation that does not get rid of EVs. This could explain why the number of EVs/RBC correlated well with haemolysis at the beginning of storage and not later. This agrees with Acker et al. and Almizraq et al. who showed positive and moderate correlations between these two parameters (Acker et al., 2018; Almizraq et al., 2018) in contrast to Tzounakas et al. who showed an inverse and very limited correlation (Tzounakas et al., 2022). Finally, since haemolysis does not reflect completely RBC status and did not differentiate the three vesiculation cohorts, particle measurement could be an interesting additional parameter for routine use. In agreement, EV abundance and RBC spherocytes (Ghodsi et al., 2023) as well as EV abundance and particles correlated better than EV with haemolysis. Nevertheless, it will be necessary to further explore this possibility by studying more RCCs in each vesiculation cohort (in particular in the high vesiculation one) at early time points.

Besides EV measurement, other RBC parameters (e.g. ATP content, morphology, deformability, plasma membrane lateral and transversal asymmetry, oxidative stress) could be considered as additional parameters to evaluate RCC quality. However, each

of them presents limitations. Regarding intracellular ATP content, it is sufficient until the end of the storage period according to the high quantity of glucose provided in bags and it does not evolve differentially in the three vesiculation cohorts during storage (Ghodsi et al., 2023). RBC membrane lateral and transversal asymmetries discriminate better between vesiculation cohorts but they develop either too late during storage (transversal asymmetry) (Ghodsi et al., 2023) or are not adapted for routine tests because they are time-consuming (lateral heterogeneity through fluorescence microscopy) (Ghodsi et al., 2023). Likewise, RBC morphology (through microscopy) and deformability (through ektacytometry) could be difficult to consider since discrimination between the different RBC sub-populations is most of the time study-dependent due to the absence of clear classification criteria and ektacytometry needs specific and expensive equipment. Regarding oxidative stress, it could represent a potential factor to be considered as it was regularly described in RCCs in the literature (D'Alessandro et al., 2012; Delobel et al., 2012; Gevi et al., 2012; Kassa et al., 2024; Kriebardis et al., 2008). However, in our previous publication, although we measured variations in reactive oxygen species (ROS) content between RCCs, we did not observe any evolution over time, either in the entire cohort or by separating the RCCs into the three vesiculation groups. Furthermore, the metHb content, a major target of ROS, was also not increased (Ghodsi et al., 2023).

The above limitations combined with the fact that the QC sampling tubing has a limited RCC volume, which could prevent these parameters from being measured, led us to propose EV measurement as a more relevant candidate. Indeed, it requires a small RCC volume (0.5 mL) and could be relatively easy to implement with the  $1,000 \times g$  protocol in the routine procedure. Moreover, EVs increase rapidly during storage, reflect the accumulation of storage lesions, and better discriminate the three vesiculation cohorts compared with ATP or haemolysis at 6w of storage (Ghodsi et al., 2023).

#### 4.6 | Application areas for particle measurement

In the long term, the implementation of our  $2,000 \times g$  protocol (adapted to  $1,000 \times g$  protocol) could help to control the conservation period of RCCs. Indeed, if an RBC unit releases many particles very quickly (high vesiculation cohort), it will provide an argument in favour of a rapid transfusion. Conversely, if few particles are released (low vesiculation cohort), the RCC could be stored longer. This will obviously require determining a threshold at which the particle abundance and/or its protein profile become problematic for RBC survival and transfusion efficiency. Furthermore, the  $2,000 \times g$  protocol could help in the context of the debate regarding the effect of the long-term versus short-term RCC storage on the transfusion safety and efficacy, specifically for at high-risk patients. In the last decades, different randomized clinical trials, meta-analyses and observational studies have been published. They tried to determine the risk of transfusing old versus fresh RCCs in different categories of patients (critically ill patients, in the intensive care unit, during cardiac surgery, in healthy adults...). However, no consensus could have been established regarding the age of RCC and its adverse outcomes after transfusion (Fergusson et al., 2012; Goel et al., 2016; Lacroix et al., 2015; Lelubre & Vincent, 2013; Wang et al., 2012). This link was suspected because of the numerous *in vitro* studies on storage lesions. Given the variability between RCCs within a storage time, our hypothesis is that storage time does not always reflect RCC quality in contrast to EV/particle release (Koch et al., 2019). A standardized, reproducible protocol for particle measurement and the use of our RCC classification into cohorts could therefore help to control the choice of bags for transfusion in order to protect patients.

Another area of application could be envisaged. It is related to the replacement of the plasticizer di(2-ethylhexyl) phthalate (DEHP) in medical devices. DEHP was shown to stabilize and maintain RBC membrane integrity, thereby reducing haemolysis during storage (Horowitz et al., 1985; Rock et al., 1984). However, it is also an endocrine-disrupting substance that has toxic effects on the environment and supposedly on health (Kim et al., 2003). For this reason, European legislation has planned to ban its use in medical devices in 2030 (Regulation EC 2023/2482 published in the Official Journal of the European Union in November 2023). A standardized and reproducible protocol for EV or particle measurement could help to better characterize the consequences of DEHP absence on RBC membrane stability and the risk for the transfusion efficacy and safety.

#### 4.7 | Study limitations

Although 70 RCCs from 68 donors were included, our study encountered some design limitations. First, most of the RCCs were not followed horizontally during storage, meaning that several time intervals did not comprise the exact same RCCs and potentially introduced donor-related issues. Nevertheless, the comparison of 6 individual RCCs (two from each cohort) followed during the whole period of storage with their respective entire vesiculation cohort (non-followed horizontally during storage) revealed similar particle exponential increases, ruling out a bias related to donor variability. Second, only 12 RCCs were studied from days 1 or 2. Therefore, early time points require further investigation. Third, by stratifying RCCs into three cohorts, the number of RCCs studied in each group (particularly in the high vesiculation group) was limited, which reduced the power of statistical analyses. Besides design limitations, the use of a segment of the QC tubing as a non-invasive technique was, to the best of our knowledge, never reported before. Moreover, this tubing is not available on all products and no data exist on potential side

effects of the stripping procedure on RBCs. Finally, measurements by NTA can also represent another limited point in our study, as discussed above. Nevertheless, we performed several complementary techniques to characterize the isolated material, such as Coomassie blue staining in gels, Western blotting and electron microscopy.

## 5 | CONCLUSION

With this study, we first highlighted the interest of using particles/EVs as a new quality control parameter in blood centres. To this end, we standardized an easy-to-use centrifugation protocol that will save time and the purchase of new equipment. Second, as already recommended by MISEV2023, we reported here that EV isolation protocols and methods must be described in a more standardized way since they influence the EV number and composition as well as the interpretation of downstream analyses (Welsh et al., 2024). Third, the variability in EV abundance observed within a storage time should be considered in future papers and our classification into three cohorts would be interesting for this purpose. Indeed, it could help to better understand EV biogenesis and to assess the impact on RBC functionality and transfusion safety. Finally, this research paves the way for using particle measurement and vesiculation cohort classification to (i) evaluate RCC quality over time in blood centres by using the QC sampling tubing in parallel to haemolysis, (ii) decipher the consequence of DEHP loss on RBC membrane stability, and (iii) launch clinical studies on the transfusion of stored RBC units.

### AUTHOR CONTRIBUTIONS

**Marine Ghodsi:** Conceptualization (equal); investigation (equal); methodology (equal); writing—original draft (equal). **Anne-Sophie Cloos:** Investigation (equal); methodology (equal); writing—review and editing (equal). **Anaïs Lotens:** Investigation (equal); methodology (equal); writing—review & editing (equal). **Marine De Bueger:** Investigation (equal); writing—review and editing (equal). **Patrick Van Der Smissen:** Investigation (equal); writing—review and editing (equal). **Patrick Henriët:** Formal analysis (equal); writing—review and editing (equal). **Nicolas Cellier:** Data curation (equal); writing—review and editing (equal). **Christophe E. Pierreux:** Formal analysis (equal); writing—review and editing (equal). **Tomé Najdovski:** Data curation (equal); writing—review and editing (equal). **Donatienne Tyteca:** Conceptualization (equal); methodology (equal); supervision (equal); writing—original draft (equal); writing—review and editing (equal).

### ACKNOWLEDGEMENTS

We would like to thank Dr. S. Horman (IREC Institute, UCLouvain) for providing us with platelet lysates as well as the Laboratoire central automatisé (Cliniques universitaires Saint-Luc) for access to the hematological equipment (Sysmex). This work was supported by grants from UCL (FSR and Actions de Recherches concertées, ARC). Some figures were created with BioRender.com

### CONFLICT OF INTEREST STATEMENT

The authors declare no competing financial interests.

### ORCID

Donatienne Tyteca  <https://orcid.org/0000-0002-7334-2648>

### REFERENCES

- Abonnenc, M., Tissot, J. D., & Prudent, M. (2018). General overview of blood products in vitro quality: Processing and storage lesions. *Transfusion Clinique Et Biologique: Journal De La Societe Francaise De Transfusion Sanguine*, 25(4), 269–275. <https://doi.org/10.1016/j.tracli.2018.08.162>
- Acker, J. P., Almizraq, R. J., Millar, D., & Maurer-Spurej, E. (2018). Screening of red blood cells for extracellular vesicle content as a product quality indicator. *Transfusion*, 58(9), 2217–2226. <https://doi.org/10.1111/trf.14782>
- Almizraq, R. J., Holovati, J. L., & Acker, J. P. (2018). Characteristics of extracellular vesicles in red blood concentrates change with storage time and blood manufacturing method. *Transfusion Medicine and Hemotherapy: Offizielles Organ Der Deutschen Gesellschaft Fur Transfusionsmedizin Und Immunhamatologie*, 45(3), 185–193. <https://doi.org/10.1159/000486137>
- Almizraq, R. J., Seghatchian, J., Holovati, J. L., & Acker, J. P. (2017). Extracellular vesicle characteristics in stored red blood cell concentrates are influenced by the method of detection. *Transfusion and Apheresis Science: Official Journal of the World Apheresis Association: Official Journal of the European Society for Haemapheresis*, 56(2), 254–260. <https://doi.org/10.1016/j.transci.2017.03.007>
- Auffray, I., Marfatia, S., de Jong, K., Lee, G., Huang, C. H., Paszty, C., Tanner, M. J., Mohandas, N., & Chasis, J. A. (2001). Glycophorin A dimerization and band 3 interaction during erythroid membrane biogenesis: In vivo studies in human glycophorin A transgenic mice. *Blood*, 97(9), 2872–2878. <https://doi.org/10.1182/blood.v97.9.2872>
- Bachurski, D., Schuldner, M., Nguyen, P. H., Malz, A., Reinert, K. S., Grenzi, P. C., Babatz, F., Schauss, A. C., Hansen, H. P., Hallek, M., & Pogge von Strandmann, E. (2019). Extracellular vesicle measurements with nanoparticle tracking analysis—An accuracy and repeatability comparison between NanoSight NS300 and ZetaView. *Journal of Extracellular Vesicles*, 8(1), 1596016. <https://doi.org/10.1080/20013078.2019.1596016>
- Bebesi, T., Kitka, D., Gaál, A., Szegvártó, I. C., Deák, R., Beke-Somfai, T., Koprivanacz, K., Juhász, T., Bóta, A., Varga, Z., & Mihály, J. (2022). Storage conditions determine the characteristics of red blood cell derived extracellular vesicles. *Scientific Reports*, 12(1), 977. <https://doi.org/10.1038/s41598-022-04915-7>

- Belzaira, R. M., Prakash, P. S., Richter, J. R., Robinson, B. R., Edwards, M. J., Caldwell, C. C., Lentsch, A. B., & Pritts, T. A. (2012). Microparticles from stored red blood cells activate neutrophils and cause lung injury after hemorrhage and resuscitation. *Journal of the American College of Surgeons*, 214(4), 648–657. <https://doi.org/10.1016/j.jamcollsurg.2011.12.032>
- Bicalho, B., Serrano, K., Dos Santos Pereira, A., Devine, D. V., & Acker, J. P. (2016). Blood bag plasticizers influence red blood cell vesiculation rate without altering the lipid composition of the vesicles. *Transfusion Medicine and Hemotherapy: Offizielles Organ Der Deutschen Gesellschaft Fur Transfusionsmedizin Und Immunhamatologie*, 43(1), 19–26. <https://doi.org/10.1159/000441639>
- Bolotta, A., Battistelli, M., Falcieri, E., Ghezzi, A., Manara, M. C., Manfredini, S., Marini, M., Posar, A., Visconti, P., & Abruzzo, P. M. (2018). Oxidative stress in autistic children alters erythrocyte shape in the absence of quantitative protein alterations and of loss of membrane phospholipid asymmetry. *Oxidative Medicine and Cellular Longevity*, 2018, 6430601. <https://doi.org/10.1155/2018/6430601>
- Bosman, G. J., Lasonder, E., Lutén, M., Roerdinkholder-Stoelwinder, B., Novotný, V. M., Bos, H., & De Grip, W. J. (2008). The proteome of red cell membranes and vesicles during storage in blood bank conditions. *Transfusion*, 48(5), 827–835. <https://doi.org/10.1111/j.1537-2995.2007.01630.x>
- Brennan, K., Martin, K., FitzGerald, S. P., O'Sullivan, J., Wu, Y., Blanco, A., Richardson, C., & Mc Gee, M. M. (2020). A comparison of methods for the isolation and separation of extracellular vesicles from protein and lipid particles in human serum. *Scientific Reports*, 10(1), 1039. <https://doi.org/10.1038/s41598-020-57497-7>
- Cloos, A. S., Ghodsi, M., Stommen, A., Vanderroost, J., Danguet, N., Pollet, H., D'Auria, L., Mignolet, E., Larondelle, Y., Terrasi, R., Muccioli, G. G., Van Der Smissen, P., & Tyteca, D. (2020). Interplay between plasma membrane lipid alteration, oxidative stress and calcium-based mechanism for extracellular vesicle biogenesis from erythrocytes during blood storage. *Frontiers in Physiology*, 11, 712. <https://doi.org/10.3389/fphys.2020.00712>
- Cvjetkovic, A., Lötval, J., & Lässer, C. (2014). The influence of rotor type and centrifugation time on the yield and purity of extracellular vesicles. *Journal of Extracellular Vesicles*, 3, 23111. <https://doi.org/10.3402/jev.v3.23111>
- D'Alessandro, A., D'Amici, G. M., Vaglio, S., & Zolla, L. (2012). Time-course investigation of SAGM-stored leukocyte-filtered red blood cell concentrates: From metabolism to proteomics. *Haematologica*, 97(1), 107–115. <https://doi.org/10.3324/haematol.2011.051789>
- D'Alessandro, A., Liembruno, G., Grazzini, G., & Zolla, L. (2010). Red blood cell storage: The story so far. *Blood Transfusion = Trasfusione Del Sangue*, 8(2), 82–88. <https://doi.org/10.2450/2009.0122-09>
- Delobel, J., Prudent, M., Rubin, O., Crettaz, D., Tissot, J. D., & Lion, N. (2012). Subcellular fractionation of stored red blood cells reveals a compartment-based protein carbonylation dynamics. *Journal of Proteomics*, 76, Spec No. 181–193. <https://doi.org/10.1016/j.jprot.2012.05.004>
- Dinkla, S., Peppelman, M., Van Der Raadt, J., Atsma, F., Novotný, V. M., Van Kraaij, M. G., Joosten, I., & Bosman, G. J. (2014). Phosphatidylserine exposure on stored red blood cells as a parameter for donor-dependent variation in product quality. *Blood Transfus*, 12(2), 204–209. <https://doi.org/10.2450/2013.0106-13>
- Dlugolecka, M., Szymanski, J., Zareba, L., Homoncik, Z., Domagala-Kulawik, J., Polubiec-Kownacka, M., & Czystowska-Kuzmicz, M. (2021). Characterization of extracellular vesicles from bronchoalveolar lavage fluid and plasma of patients with lung lesions using fluorescence nanoparticle tracking analysis. *Cells*, 10(12), 3473. <https://doi.org/10.3390/cells10123473>
- Fergusson, D. A., Hébert, P., Hogan, D. L., LeBel, L., Rouvinez-Bouali, N., Smyth, J. A., Sankaran, K., Tinmouth, A., Blajchman, M. A., Kovacs, L., Lachance, C., Lee, S., Walker, C. R., Hutton, B., Ducharme, R., Balchin, K., Ramsay, T., Ford, J. C., Kakadekar, A., ... Shapiro, S. (2012). Effect of fresh red blood cell transfusions on clinical outcomes in premature, very low-birth-weight infants: The ARIPI randomized trial. *Jama*, 308(14), 1443–1451. <https://doi.org/10.1001/2012.jama.11953>
- Fischer, D., Büsow, J., Meybohm, P., Weber, C. F., Zacharowski, K., Urbschat, A., Müller, M. M., & Jennewein, C. (2017). Microparticles from stored red blood cells enhance procoagulant and proinflammatory activity. *Transfusion*, 57(11), 2701–2711. <https://doi.org/10.1111/trf.14268>
- Freitas Leal, J. K., Lasonder, E., Sharma, V., Schiller, J., Fanelli, G., Rinalducci, S., Brock, R., & Bosman, G. (2020). Vesiculation of red blood cells in the blood bank: A multi-omics approach towards identification of causes and consequences. *Proteomes*, 8(2), 6. <https://doi.org/10.3390/proteomes8020006>
- Gamonet, C., Desmarests, M., Mourey, G., Biichle, S., Aupet, S., Laheurte, C., François, A., Resch, E., Bigey, F., Binda, D., Bardiaux, L., Naegelen, C., Marpoux, N., Delettre, F. A., Saas, P., Morel, P., Tiberghien, P., Lacroix, J., Capellier, G., ... Garnache-Ottou, F. (2020). Processing methods and storage duration impact extracellular vesicle counts in red blood cell units. *Blood Advances*, 4(21), 5527–5539. <https://doi.org/10.1182/bloodadvances.2020001658>
- Gamonet, C., Mourey, G., Aupet, S., Biichle, S., Petitjean, R., Vidal, C., Pugin, A., Naegelen, C., Tiberghien, P., Morel, P., Angelot-Delettre, F., Seilles, E., Saas, P., Bardiaux, L., & Garnache-Ottou, F. (2017). How to quantify microparticles in RBCs? A validated flow cytometry method allows the detection of an increase in microparticles during storage. *Transfusion*, 57(3), 504–516. <https://doi.org/10.1111/trf.13989>
- García-Roa, M., Del, C., Vicente-Ayuso, M., Bobes, A. M., Pedraza, A. C., González-Fernández, A., Martín, M. P., Sáez, I., Seghatchian, J., & Gutiérrez, L. (2017). Red blood cell storage time and transfusion: Current practice, concerns and future perspectives. *Blood Transfusion = Trasfusione Del Sangue*, 15(3), 222–231. <https://doi.org/10.2450/2017.0345-16>
- Gevi, F., D'Alessandro, A., Rinalducci, S., & Zolla, L. (2012). Alterations of red blood cell metabolome during cold liquid storage of erythrocyte concentrates in CPD-SAGM. *Journal of Proteomics*, 76, Spec No. 168–180. <https://doi.org/10.1016/j.jprot.2012.03.012>
- Ghodsi, M., Cloos, A. S., Mozaheb, N., Van Der Smissen, P., Henriët, P., Pierreux, C. E., Cellier, N., Mingeot, M. P., Najdovski, T., & Tyteca, D. (2023). Variability of extracellular vesicle release during storage of red blood cell concentrates is associated with differential membrane alterations, including loss of cholesterol-enriched domains. *Frontiers in Physiology*, 14, 1205493. <https://doi.org/10.3389/fphys.2023.1205493>
- Goel, R., Johnson, D. J., Scott, A. V., Tobian, A. A., Ness, P. M., Nagababu, E., & Frank, S. M. (2016). Red blood cells stored 35 days or more are associated with adverse outcomes in high-risk patients. *Transfusion*, 56(7), 1690–1698. <https://doi.org/10.1111/trf.13559>
- Hadjesfandiari, N., Khorshidfar, M., & Devine, D. V. (2021). Current understanding of the relationship between blood donor variability and blood component quality. *International Journal of Molecular Sciences*, 22(8), 3943. <https://doi.org/10.3390/ijms22083943>
- Hashemi Tayer, A., Amirizadeh, N., Ahmadinejad, M., Nikougoftar, M., Deyhim, M. R., & Zolfaghari, S. (2019). Procoagulant activity of red blood cell-derived microvesicles during red cell storage. *Transfusion Medicine and Hemotherapy: Offizielles Organ Der Deutschen Gesellschaft Fur Transfusionsmedizin Und Immunhamatologie*, 46(4), 224–230. <https://doi.org/10.1159/000494367>
- He, Y., Song, H. D., Anantharamaiah, G. M., Palgunachari, M. N., Bornfeldt, K. E., Segrest, J. P., & Heinecke, J. W. (2019). Apolipoprotein A1 forms 5/5 and 5/4 antiparallel dimers in human high-density lipoprotein. *Molecular & Cellular Proteomics: MCP*, 18(5), 854–864. <https://doi.org/10.1074/mcp.RA118.000878>
- HealthCare EDftQoM. (2023). Guide to the preparation, use and quality assurance of blood components. Council of Europe Pub., 2003.
- Hess, J. R., Sparrow, R. L., van der Meer, P. F., Acker, J. P., Cardigan, R. A., & Devine, D. V. (2009). Red blood cell hemolysis during blood bank storage: Using national quality management data to answer basic scientific questions. *Transfusion*, 49(12), 2599–2603. <https://doi.org/10.1111/j.1537-2995.2009.02275.x>
- Horowitz, B., Stryker, M. H., Waldman, A. A., Woods, K. R., Gass, J. D., & Drago, J. (1985). Stabilization of red blood cells by the plasticizer, diethylhexylphthalate. *Vox Sanguinis*, 48(3), 150–155. <https://doi.org/10.1111/j.1423-0410.1985.tb00162.x>
- Kashkanova, A. D., Blessing, M., Reischke, M., Baur, J. O., Baur, A. S., Sandoghdar, V., & Van Deun, J. (2023). Label-free discrimination of extracellular vesicles from large lipoproteins. *Journal of Extracellular Vesicles*, 12(8), e12348. <https://doi.org/10.1002/jev.12348>

- Kassa, T., Jana, S., Baek, J. H., & Alayash, A. I. (2024). Impact of cold storage on the oxygenation and oxidation reactions of red blood cells. *Frontiers in Physiology*, 15, 1427094. <https://doi.org/10.3389/fphys.2024.1427094>
- Kim, H. S., Saito, K., Ishizuka, M., Kazusaka, A., & Fujita, S. (2003). Short period exposure to di-(2-ethylhexyl) phthalate regulates testosterone metabolism in testis of prepubertal rats. *Archives of Toxicology*, 77(8), 446–451. <https://doi.org/10.1007/s00204-003-0466-7>
- Klei, T. R. L., Begue, S., Lotens, A., Sigurjónsson, Ó. E., Wiltshire, M. D., George, C., van den Burg, P. J. M., Evans, R., Larsson, L., Thomas, S., Najdovski, T., Handke, W., Eronen, J., Mallas, B., & de Korte, D. (2023). Recommendations for in vitro evaluation of blood components collected, prepared and stored in non-DEHP medical devices. *Vox Sanguinis*, 118(2), 165–177. <https://doi.org/10.1111/vox.13384>
- Koch, C. G., Duncan, A. I., Figueroa, P., Dai, L., Sessler, D. I., Frank, S. M., Ness, P. M., Mihaljevic, T., & Blackstone, E. H. (2019). Real age: Red blood cell aging during storage. *Ann Thorac Surg*, 107(3), 973–980. <https://doi.org/10.1016/j.athoracsurg.2018.08.073>
- Kozlova, E., Chernysh, A., Moroz, V., Kozlov, A., Sergunova, V., Sherstyukova, E., & Gudkova, O. (2021). Two-step process of cytoskeletal structural damage during long-term storage of packed red blood cells. *Blood Transfus*, 19(2), 124–134. <https://doi.org/10.2450/2020.0220-20>
- Kriebardis, A. G., Antonelou, M. H., Stamoulis, K. E., Economou-Petersen, E., Margaritis, L. H., & Papassideri, I. S. (2008). RBC-derived vesicles during storage: Ultrastructure, protein composition, oxidation, and signaling components. *Transfusion*, 48(9), 1943–1953. <https://doi.org/10.1111/j.1537-2995.2008.01794.x>
- Lacroix, J., Hébert, P. C., Fergusson, D. A., Timmouth, A., Cook, D. J., Marshall, J. C., Clayton, L., McIntyre, L., Callum, J., Turgeon, A. F., Blajchman, M. A., Walsh, T. S., Stanworth, S. J., Campbell, H., Capellier, G., Tiberghien, P., Bardiaux, L., van de Watering, L., van der Meer, N. J., ... Canadian Critical Care Trials Group. (2015). Age of transfused blood in critically ill adults. *The New England Journal of Medicine*, 372(15), 1410–1418. <https://doi.org/10.1056/NEJMoa1500704>
- Laurén, E., Tigistu-Sahle, F., Valkonen, S., Westberg, M., Valkeajärvi, A., Eronen, J., Siljander, P., Pettilä, V., Käkälä, R., Laitinen, S., & Kerkelä, E. (2018). Phospholipid composition of packed red blood cells and that of extracellular vesicles show a high resemblance and stability during storage. *Biochimica Et Biophysica Acta. Molecular and Cell Biology of Lipids*, 1863(1), 1–8. <https://doi.org/10.1016/j.bbalip.2017.09.012>
- Lelubre, C., & Vincent, J. L. (2013). Relationship between red cell storage duration and outcomes in adults receiving red cell transfusions: A systematic review. *Critical Care (London, England)*, 17(2), R66. <https://doi.org/10.1186/cc12600>
- Li, K., Wong, D. K., Luk, F. S., Kim, R. Y., & Raffai, R. L. (2018). Isolation of plasma lipoproteins as a source of extracellular RNA. *Methods in Molecular Biology (Clifton, N.J.)*, 1740, 139–153. [https://doi.org/10.1007/978-1-4939-7652-2\\_11](https://doi.org/10.1007/978-1-4939-7652-2_11)
- Ma, S. R., Xia, H. F., Gong, P., & Yu, Z. L. (2023). Red blood cell-derived extracellular vesicles: An overview of current research progress, challenges, and opportunities. *Biomedicines*, 11(10), 2798. <https://doi.org/10.3390/biomedicines11102798>
- McNicholas, K., Li, J. Y., Michael, M. Z., & Gleadle, J. M. (2017). Albuminuria is not associated with elevated urinary vesicle concentration but can confound nanoparticle tracking analysis. *Nephrology (Carlton, Vic.)*, 22(11), 854–863. <https://doi.org/10.1111/nep.12867>
- Momen-Heravi, F., Balaj, L., Alian, S., Mantel, P. Y., Halleck, A. E., Trachtenberg, A. J., Soria, C. E., Oquin, S., Bonebreak, C. M., Saracoglu, E., Skog, J., & Kuo, W. P. (2013). Current methods for the isolation of extracellular vesicles. *Biological Chemistry*, 394(10), 1253–1262. <https://doi.org/10.1515/hsz-2013-0141>
- Nieuwland, R., & Siljander, P. R. (2024). A beginner's guide to study extracellular vesicles in human blood plasma and serum. *Journal of Extracellular Vesicles*, 13(1), e12400. <https://doi.org/10.1002/jev2.12400>
- Rock, G., Tocchi, M., Ganz, P. R., & Tackaberry, E. S. (1984). Incorporation of plasticizer into red cells during storage. *Transfusion*, 24(6), 493–498. <https://doi.org/10.1046/j.1537-2995.1984.24685066808.x>
- Rother, R. P., Bell, L., Hillmen, P., & Gladwin, M. T. (2005). The clinical sequelae of intravascular hemolysis and extracellular plasma hemoglobin: A novel mechanism of human disease. *Jama*, 293(13), 1653–1662. <https://doi.org/10.1001/jama.293.13.1653>
- Roussel, C., Dussiot, M., Marin, M., Morel, A., Ndour, P. A., Duez, J., Le Van Kim, C., Hermine, O., Colin, Y., Buffet, P. A., & Amireault, P. (2017). Spherocytic shift of red blood cells during storage provides a quantitative whole cell-based marker of the storage lesion. *Transfusion*, 57(4), 1007–1018. <https://doi.org/10.1111/trf.14015>
- Rubin, O., Canellini, G., Delobel, J., Lion, N., & Tissot, J. D. (2012). Red blood cell microparticles: Clinical relevance. *Transfusion Medicine and Hemotherapy: Offizielles Organ Der Deutschen Gesellschaft Fur Transfusionsmedizin Und Immunhamatologie*, 39(5), 342–347. <https://doi.org/10.1159/000342228>
- Rubin, O., Cretaz, D., Canellini, G., Tissot, J. D., & Lion, N. (2008). Microparticles in stored red blood cells: An approach using flow cytometry and proteomic tools. *Vox Sanguinis*, 95(4), 288–297. <https://doi.org/10.1111/j.1423-0410.2008.01101.x>
- Rubin, O., Delobel, J., Prudent, M., Lion, N., Kohl, K., Tucker, E. I., Tissot, J. D., & Angelillo-Scherrer, A. (2013). Red blood cell-derived microparticles isolated from blood units initiate and propagate thrombin generation. *Transfusion*, 53(8), 1744–1754. <https://doi.org/10.1111/trf.12008>
- Serrano-Pertierra, E., Oliveira-Rodríguez, M., Matos, M., Gutiérrez, G., Moyano, A., Salvador, M., Rivas, M., & Blanco-López, M. C. (2020). Extracellular vesicles: Current analytical techniques for detection and quantification. *Biomolecules*, 10(6), 824. <https://doi.org/10.3390/biom10060824>
- Sharifian Gh, M., & Norouzi, F. (2023). Guidelines for an optimized differential centrifugation of cells. *Biochemistry and Biophysics Reports*, 36, 101585. <https://doi.org/10.1016/j.bbrep.2023.101585>
- Sowemimo-Coker, S. O. (2002). Red blood cell hemolysis during processing. *Transfusion Medicine Reviews*, 16(1), 46–60. <https://doi.org/10.1053/tmr.2002.29404>
- Stam, J., Bartel, S., Bischoff, R., & Wolters, J. C. (2021). Isolation of extracellular vesicles with combined enrichment methods. *Journal of Chromatography. B, Analytical Technologies in the Biomedical and Life Sciences*, 1169, 122604. <https://doi.org/10.1016/j.jchromb.2021.122604>
- Takov, K., Yellon, D. M., & Davidson, S. M. (2018). Comparison of small extracellular vesicles isolated from plasma by ultracentrifugation or size-exclusion chromatography: Yield, purity and functional potential. *Journal of Extracellular Vesicles*, 8(1), 1560809. <https://doi.org/10.1080/20013078.2018.1560809>
- Théry, C., Amigorena, S., Raposo, G., & Clayton, A. (2006). Isolation and characterization of exosomes from cell culture supernatants and biological fluids. *Current protocols in cell biology, Chapter 3*. <https://doi.org/10.1002/0471143030.cb0322s30>
- Théry, C., Witwer, K. W., Aikawa, E., Alcaraz, M. J., Anderson, J. D., Andriantsitohaina, R., Antoniou, A., Arab, T., Archer, F., Atkin-Smith, G. K., Ayre, D. C., Bach, J. M., Bachurski, D., Baharvand, H., Balaj, L., Baldacchino, S., Bauer, N. N., Baxter, A. A., Bebawy, M., ... Zuba-Surma, E. K. (2018). Minimal information for studies of extracellular vesicles 2018 (MISEV2018): A position statement of the International Society for Extracellular Vesicles and update of the MISEV2014 guidelines. *Journal of Extracellular Vesicles*, 7(1), 1535750. <https://doi.org/10.1080/20013078.2018.1535750>
- Tripisciano, C., Weiss, R., Karuthedom George, S., Fischer, M. B., & Weber, V. (2020). Extracellular vesicles derived from platelets, red blood cells, and monocyte-like cells differ regarding their ability to induce factor XII-dependent thrombin generation. *Frontiers in Cell and Developmental Biology*, 8, 298. <https://doi.org/10.3389/fcell.2020.00298>
- Tzounakas, V. L., Anastasiadi, A. T., Lekka, M. E., Papageorgiou, E. G., Stamoulis, K., Papassideri, I. S., Kriebardis, A. G., & Antonelou, M. H. (2022). Deciphering the relationship between free and vesicular hemoglobin in stored red blood cell units. *Frontiers in Physiology*, 13, 840995. <https://doi.org/10.3389/fphys.2022.840995>
- van der Pol, E., Coumans, F., Varga, Z., Krumrey, M., & Nieuwland, R. (2013). Innovation in detection of microparticles and exosomes. *Journal of Thrombosis and Haemostasis: JTH*, 11(Suppl. 1), 36–45. <https://doi.org/10.1111/jth.12254>

- Wang, D., Sun, J., Solomon, S. B., Klein, H. G., & Natanson, C. (2012). Transfusion of older stored blood and risk of death: A meta-analysis. *Transfusion*, 52(6), 1184–1195. <https://doi.org/10.1111/j.1537-2995.2011.03466.x>
- Wasan, K. M., Brocks, D. R., Lee, S. D., Sachs-Barrable, K., & Thornton, S. J. (2008). Impact of lipoproteins on the biological activity and disposition of hydrophobic drugs: Implications for drug discovery. *Nature Reviews. Drug Discovery*, 7(1), 84–99. <https://doi.org/10.1038/nrd2353>
- Welsh, J. A., Goberdhan, D. C. I., O'Driscoll, L., Buzas, E. I., Blenkiron, C., Bussolati, B., Cai, H., Di Vizio, D., Driedonks, T. A. P., Erdbrügger, U., Falcon-Perez, J. M., Fu, Q. L., Hill, A. F., Lenassi, M., Lim, S. K., Mahoney, M. G., Mohanty, S., Möller, A., Nieuwland, R., ... Witwer, K. W. (2024). Minimal information for studies of extracellular vesicles (MISEV2023): From basic to advanced approaches. *Journal of Extracellular Vesicles*, 13(2), e12404. <https://doi.org/10.1002/jev2.12404>
- Yoshida, T., Prudent, M., & D'alessandro, A. (2019). Red blood cell storage lesion: Causes and potential clinical consequences. *Blood Transfusion = Trasfusione Del Sangue*, 17(1), 27–52. <https://doi.org/10.2450/2019.0217-18>
- Zimmerman, A. J., de Oliveira, G. P., Jr, Su, X., Wood, J., Fu, Z., Pinckney, B., Tigges, J., Ghiran, I., & Ivanov, A. R. (2024). Multimode chromatography-based techniques for high purity isolation of extracellular vesicles from human blood plasma. *Journal of Extracellular Biology*, 3(3), e147. <https://doi.org/10.1002/jex2.147>
- Zimring, J. C. (2015). Established and theoretical factors to consider in assessing the red cell storage lesion. *Blood*, 125(14), 2185–2190. <https://doi.org/10.1182/blood-2014-11-567750>

## SUPPORTING INFORMATION

Additional supporting information can be found online in the Supporting Information section at the end of this article.

**How to cite this article:** Ghodsi, M., Cloos, A.-S., Lotens, A., De Bueger, M., Van Der Smissen, P., Henriët, P., Cellier, N., Pierreux, C. E., Najdovski, T., & Tyteca, D. (2025). Development of an easy non-destructive particle isolation protocol for quality control of red blood cell concentrates. *Journal of Extracellular Biology*, 4, e70028. <https://doi.org/10.1002/jex2.70028>